Dissertations, Master's Theses and Master's Reports - Open

Dissertations, Master's Theses and Master's Reports

2012

Electrospun chitosan nanofibers for virus removal

Bingyu Bai
Michigan Technological University

Recommended Citation

ELECTROSPUN CHITOSAN NANOFIBERS FOR VIRUS REMOVAL

By

Bingyu Bai

A THESIS

Submitted in partial fulfillment of the requirements for the degree of

MASTER OF SCIENCE

(Chemical Engineering)

MICHIGAN TECHNOLOGICAL UNIVERSITY

2012

This thesis, "Electrospun Chitosan Nanofibers for Virus Removal," is hereby approved in partial fulfillment of the requirements for the Degree of MASTER OF SCIENCE IN CHEMICAL ENGINEERING.

Department of Chemical Engineering

Signatures:

Thesis Advisor   _____

Dr. Caryn Heldt

Committee Member   _____

Dr. Patricia A.Heiden

   _____

Dr. Ching An-Peng

   _____

Dr. Genard T. Caneba

Department Chair   _____

Dr. Komar Kawatra

Date   _____

Table of Contents

List of Figures

List of tables

Acknowledgements

I would like to thank my advisor, Dr. Caryn Heldt, for her constant support and help and NSF for funding.

I would like to thank my committee members, Dr.Heiden, Dr.Peng, Dr.Caneba, for their insights and help in the preparation of this thesis. I would like to thank my entire lab mates for their help. I would like to thank Dr.Heiden's entire lab, for their technical support. I would like to thank Xiang Xu for helping me with NMR and for his gift of graphene and Ning Chen for training me on electrospinning techniques.

Finally, I would like to thank my parents and my boyfriend Brian Feng, for their support and their love.

Abbreviations

DD — Degree of deacetylation

DQ — Degree of quaternization

FCV-F9 — Feline calicivirus F9

GTMAC — Glycidyl-trimethylammonium chloride

HTCC — N-[(2-hydroxy-3-trimethylammonium) propyl] chitosan chloride

LRV — Log reduction value

MBC — Minimum bactericidal concentration

MF — Microfiltration

MIC — Minimum inhibitory concentration

MNV-1 — Murine norovirus

MWCO — Molecular weight cut off

PAN — Polyacrylonitrile

PBS — Phosphate-buffered saline

PDLA — Poly (D-lactide)

PET — Polyethylene terephthalate

PEVA — Poly (ethylene-co-vinyl acetate)

PFU — Plaque forming units

PK-13 — Porcine kidney cells

PLA — Poly (lactic acid)

PLGA — Poly (lactic-co-glycolic acid)

PLLA — Poly (L-lactic acid)

POE — Poly (oxyethylene)

PPV   - Porcine parvovirus

PS   - Polystyrene

PVA   - Poly (vinyl alcohol)

SDS   - Sodium dodecyl sulfate

SLPF   - Silk-like polymer with fibronectin

UF   - Ultrafiltration

UHMWPEO - Ultrahigh-molecular-weight poly (ethylene oxide)

Abstract

Electrospinning uses electrostatic forces to create nanofibers that are far smaller than conventional fiber spinning process. Nanofibers made with chitosan were created and techniques to control fibers diameter and were well developed. However, the adsorption of porcine parvovirus (PPV) was low. PPV is a small, nonenveloped virus that is difficult to remove due to its size, 18-26 nm in diameter, and its chemical stability. To improve virus adsorption, we functionalized the nanofibers with a quaternized amine, forming N-[(2-hydroxy-3-trimethylammonium) propyl] chitosan chloride (HTCC). This was blended with additives to increase the ability to form HTCC nanofibers. The additives changed the viscosity and conductivity of the electrospinning solution. We have successfully synthesized and functionalized HTCC nanofibers that absorb PPV. HTCC blend with graphene have the ability to remove a minimum of 99% of PPV present in solution.

1 Introduction

According to WHO, the lack of access to safe drinking water is of great public concern. Diarrhoeal diseases are currently responsible for about 90% of all deaths of children under five years in developing countries (WHO/UNICEF, 2010). Between 2000 and 2003,769,000 and 683,000 children less than five years of age died in sub-Saharan Africa and South Asia, respectively, each year from diarrhoeal diseases (WHO/UNICEF, 2010). Effective water purification is needed to provide an easy and inexpensive way to produce clean water.

Pathogens are microscopic biological organisms in drinking water that can cause diseases. Pathogens include virus, bacteria and protozoa (Bennett 2008). We are focusing this work on removing virus from drinking water.

Traditional filtration methods can only filter virus over 40 nm by series filtration of Planova 35 filter (pore size 35 nm; Asahi Chemical Industry, Tokyo, Japan) (Troccoli et al. 1998). But for small virus, like porcine parvovirus (PPV), traditional filtration fails to remove them completely and easily. PPV is a common model to examine virus clearance. PPV has a small diameter (18-26 nm) and is a non-enveloped virus (Simpson et al. 2002). PPV is also hard to inactivate (Kempf et al. 2007). When using small pore size nanofiltration to remove virus, difficulties include increased filter fouling, high transmembrane pressure and low water flux (Kim and Van der Bruggen 2010).

Microfiltration (MF) and ultrafiltration (UF) membranes are an advanced filtration method. Compared to traditional filtration methods, they have the ability to remove pathogens include virus and bacterial (Brehant 2008). Research has confirmed that ultrafiltration using defect free nanofibers can obtain effective removal of pathogens. The log reduction value (LRV) was between 4 and 7 for Giardia and Cryptosporidium (protozoan) after filtration with a 0.1 μm filters (Brehant 2008). Positively charged nanofibers have the ability to remove several LRV of virus (Riordan et al. 2009).

In our search for a material that has a positive charge and produces nanofibers, we decided to work with chitosan. Chitosan and chitin have gained a lot of interest in the past few years. It is considered a promising natural polymer for a lot of bio-applications, including bioseperation (Davis et al. 2012).

Chitin, poly (b-(1-4)-N-acetyl-D-glucosamine) is found in the shells of many sea organisms. Every year, large amounts of chitin are used and synthesized. It is the second most abundant polymer on earth, following cellulose (Homayoni et al. 2009). When chitin is deacetylated, it forms chitin derivatives, one of which is chitosan, whose application is the most common in the world. The most important properties of chitosan are molecular weight and DD (degree of deacetylation) (Homayoni et al. 2009). One of the characteristics that we are most interested in is that chitosan is a cationic polymer (Rinaudo 2006). To increase the cationic charge on chitosan, a quaternary ammonium derivative can be created and it is known for its antimicrobial activity against a variety of bacteria and fungi (Alipour et al. 2009).

Electrospinning is a technology that applies an external electric force to produce various nanofibers from polymer solution with a diameter changed from several nanometers to micrometers. We chose this method to create nanofibers because fiber diameters can be well controlled. When the voltage is increased, the electrostatic force will increase until the polymer surface tension is overcome, allowing a charged jet of polymer to escape from the tip of needle and travel to the collector. The ejected jet can develop a whipping motion that allows the solvent to evaporate, so fibers can form. The produced fibers diameter can be controlled by electrospinning variables, including viscosity, concentration, surface tension, conductivity, distance between the needle and collector and the polymer feed rate (Huang et al. 2003).

This study describes the preparation of nanofibers from chitosan and (N-[(2-hydroxy-3-trimethylammonium) propyl] chitosan chloride) (HTCC), via electrospinning. This thesis begins with an introduction. Chapter 2 contains a literature review. Materials and methods are covered in Chapter 3. The experiment result and discussion of our work

with chitosan and HTCC are presented in Chapter 4. Chapter 5 completes the work with our conclusions and recommendations.

Our goal was to create functionalized nanofibers that have the ability to absorb virus with large pore-sized nanofibers filters. These nanofibers filters have the advantage of increasing the flow rate and reducing fouling. These nanofibers are made from biocompatible, inexpensive and environmentally-friendly chitosan. Chitosan has the ability to be functionalized to increase its disinfection capacity. Nanofibers have an increased surface area to volume ratio as compare to microfibers and are also on the same size scale as virus, creating a curved surface that has the potential to increase virus adsorption.

In this study, we use a model non-enveloped virus porcine parvovirus (PPV). PPV is negative charged (Weichert et al. 1998), and we synthesized HTCC cationic nanofibers that have an increased positively charge, as compare to chitosan. The nanofibers made from HTCC blends have the ability to remove 99% of PPV from solution. This demonstrates that HTCC nanofibers have the potential to be used for other virus and remove pathogens from drinking water.

2 Literature Review

2.1 Biological application of nanofibers

Recently, electrospun polymer nanofibers have received a lot of interest in biologically relevant fields. Through careful control of electrospinning process parameters, various diameters of nanofibers, ranging from nanometer to micrometer, can be produced. These fibers are easy to fabricate and produce, compared to the traditional wet-spinning method. The unique ability has allowed people to apply electrospun fibers to a variety of applications. Some of these applications can be found in Fig. 2.1.

Life Science
Drug delivery
Wound dressing
Scafford for
enzyme and tissues

Polymer nanofibers

Filtration
Liquid filtration
Gas filtration
Molecular filtration

Nano-sensors
Thermal sensor
Biochemical sensor
Chemical sensor
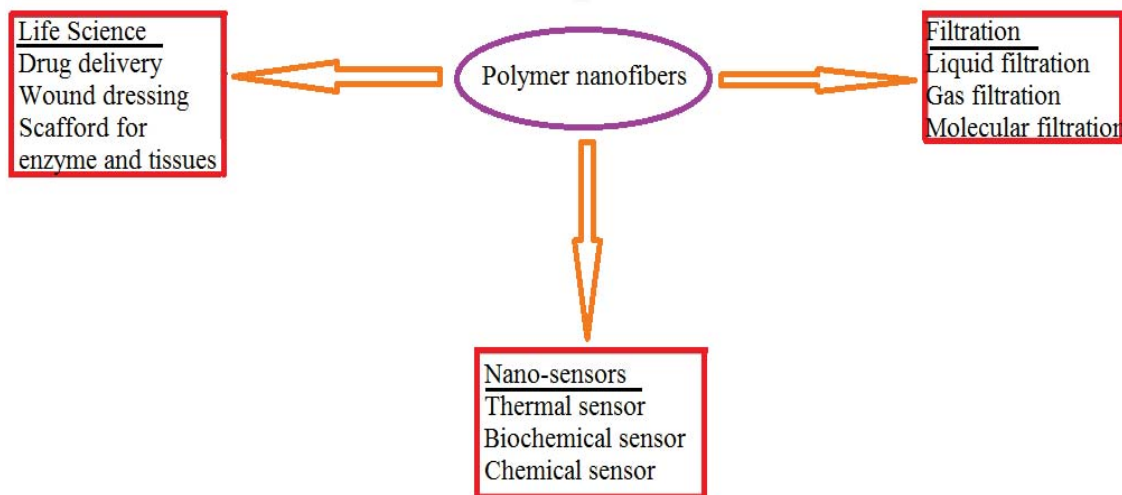
Figure 2.1 Applications of electrospun polymer nanofibers (Fang et al. 2011)

2.1.1 *In Vivo* Applications

Drug delivery using electrospun fibers represent a novel approach to controlled drug release by producing fibers with simple equipment. An effective drug release process can be produced when drugs are electrospun with biodegradable polymers. The biodegradable polymers in a fiber format provided a possibility of smooth release of drug and reduced burst release of drug by controlling the diameter of fibers (Meinel et al.

2002). By controlling the parameter of the electrospinning process, it is possible to modify the drug release kinetics and prolong drug release (Meinel et al. 2002, Kenawy et al. 2002). The release of various concentrations of tetracycline hydrochloride, an antibiotic, was studied. Electrospun drug with poly (lactic acid) (PLA) and poly (ethylene-co-vinyl acetate) (PEVA) (1:1) brought about a smooth release of drug, compared to the release of pure tetracycline hydrochloride (Kenawy et al. 2002, Kenawy et al. 2003). A maximum of 50 wt% tetracycline hydrochloride content could be used. Any higher concentration of drug brought about a reduction in the bending instability and uniformity of the fibers (Kenawy et al. 2003). Poly (L-lactic acid) (PLLA) fibers captured rifampin (a drug for tuberculosis), and paclitaxel (an anti-cancer drug) (Zeng et al. 2003). Adding different charged surfactants can decrease the fiber diameter, and therefore affect the drug release kinetics. In the presence of proteinase K, the drug can be released with zero-order kinetics, inhibiting burst release (Zeng et al. 2003). Electrospinning polymer/drug blends have been patented to a method of control drug release. Besides controlled release, the method also made insoluble drugs soluble (Ignatious 2006).

Electrospun nanofibers have been used widely in the tissue engineering field. The goal of tissue engineering is to regenerate and fabricate damaged tissue and organs by providing a scaffold that promotes cell attachment and proliferation. One of the challenges is finding an appropriate material that is biocompatible and cannot react with other tissues in the human body. Electrospinning can provide a much simpler method to produce composite scaffold with a small range in the fiber diameter (Barnes et al. 2007). After seeding cells onto 50:50 poly (L-lactic acid/caprolactone) fibers, human umbilical vein endothelial cells showed better proliferation properties than cells without fibers present. After attaching to electrospun fibers, cells become rounded and spread around the fibers (Geng et al. 2005). Similar cell proliferation has been demonstrated with mouse cells on a poly-lactic-glycolic acid (PLGA) system (Li et al. 2002).

Electrospun fibers can also be applied for wound dressing with a porous sheet-like structure. Jin et al. studied electrospun silkworm silk for wound dressing (Jin et al. 2002). Due to the nano-scale diameter of the fibers, high surface area was achieved in a small volume. The principle is that biodegradable polymers which have a high surface area can

protect the wound and help new skin to grow quicker and reduce the formation of scars, compared to a typical macro scale dressing (Jin et al. 2002).

2.1.2 Air filtration

Another important field for electrospun fibers is filtration. Electrospun fibers provide a new and effective method to remove contaminates with high filtration efficiency and low air resistance as compared to other nonwoven filters. Electrospun poly (ethylene oxide), poly (vinyl alcohol), and polyamide-6 solution deposited on PET microfibers at a filter size of 15×15 cm were tested for air permeability (Dotti et al. 2007). The pore size ranged from 0.1-1μm². Electrospun filter media showed lower resistance compared to normal macrofiltration methods, while removing particles in the submicron range. By changing the thickness of nanofibers, it is possible to control air permeability (Dotti et al. 2007). Because electrospun nanofibers have a high surface area to volume ratio and a corresponding high surface cohesion, electrospun nanofibers can remove particles as small as 0.5μm. NaCl aerosol particles were removed with 0.6 μm diameter fibers (Qin et al. 2008). Smaller electrospun nanofibers can achieve higher filtration efficiency. One issue that can be detrimental to the use of nanofibers as a filtration media is the strength of the fibers. However, crosslinking electrospun nanofibers can increase the strength of nanofibers (Qin et al. 2008).

2.1.3 Water purification

Water purification focuses on the removal of pathogens, chemicals, and heavy metals to produce clean drinking water. Various polymer solutions and polymer gels had been electrospun to try and remove these contaminates; the most common polymers are chitin (McManus et al. 2007), chitosan derivative (Alipour et al. 2009), poly (ethylene-co-vinyl alcohol) (Chuangchote et al. 2006), poly (glycolic acid) and chitin (Park et al. 2006) and chitosan/PVA (Zhang et al. 2007).

Chitosan and its derivatives have gained a lot of interest in recent years due to the wide range of applications in biomedicine, bioseperation and food science. We have,

therefore, chosen to concentrate our work on chitosan. Chitosan, the deacetylated product of chitin (produced from the crust of crustacean shells), is a bio-friendly, bio-degradable and anti-bacterial compound (Inmaculada et al. 2009). Chitosan and chitin have been shown to remove metals and dyes so that they can be used to clean water (Crini 2005). This is due to the adsorption of the metals and dyes to the cationic amine functional groups on chitosan. Various crosslinked polysaccharide materials with chitosan can remove different metal and dye pollutants (Crini 2005).

Compared to chitosan, chitin has the ability to remove polycyclic aromatic hydrocarbons more effectively (Crisafully 2008). The degree of deacetylation (DD) can affect the removal of particles like As $^{+5}$ (arsenic). Crystallinity also plays an important role in adsorption and removal of particles in water. Crystallinity is increased by the amine group that forms a hydrogen bond to other chitosan monomers, and this affects the fiber morphology and adsorption (Rinaudo et al. 2006). Chitosan can remove negatively charged dye like Reactive Black 5. Chitosan is positively charged in an acid environment, and electrostatic forces are responsible for dye removal. According to the results, changing the molecular weight (MW) of chitosan from 80,100 to 308,300 reduces chitosan's ability to adsorb dye (Guibal and Roussy 2007, Guibal et al. 2006). The reason for this can be a change in the internal structure of the chitosan chains, hydrogen bonding between hydroxyl and amine groups reduced the possibility of dye binding. Studies have found that the number of amine groups, determined by the DD, affected the removal of metal ions in water. Higher DD (97%) produced higher removal efficiency, comparing to chitosan with 52% DD (Guibal 2004, Guibal et al. 2006).

Chitosan also has anti-viral properties. We can measure the removal of virus from a solution using the log reduction value (LRV). This value is defined as the log_{10} (C_{in}/C_{out}), where C_{in} is the concentration of virus before the removal step and C_{out} is the concentration of virus after the removal step. An LRV of 1 demonstrates that 90% of the virus has been removed and an LRV of 4 represents 99.9 % removal. The virus removal step should obtain a minimum of 4 LRV according to the EPA and the FDA. A series of experiments with 0.7% chitosan in acetic acid were conducted with 5 log_{10} PFU (plaque forming units)/ml of two different nonenveloped virus (feline calicivirus F9 (FCV-F9))

and murine norovirus (MNV-1)). The results showed that chitosan can reduce FCV-F9 by 2 LRV (99%) and reduce MNV-1 by 0.7 LRV (63%) (Davis et al. 2012).

2.2 Virus Removal Techniques

According to the World Health Organization (WHO), it has reported that over one billion people do not have access to clean water (WHO/UNICEF 2010). Unsafe water often contains pathogens that can transmit diseases. Cholera, infectious hepatitis, and typhoid are some of the most common of these diseases (Bennett 2008). The people most affected are women and children in undeveloped countries. Viruses are one source of disease, even when present in very low concentrations. Clean and safe water is a basic necessity for populations to develop and thrive. This requires the development of sustainable water disinfection systems that can be applied worldwide. Traditional water filtration systems include physical filtration and chemical disinfection. The chemical disinfection method is most commonly free chlorine. The physical filtration method removes sediment and particles only based on pore size.

Worldwide, microfiltration (MF) and ultrafiltration (UF) membrane are the most common physical filtration method for drinking water purification. MF and UF membranes with 300-400 ft^2 surface area filtered 2 million m^3/d of river water (Delgrange et al. 2000). Over 74 % of clean water is produced by ultrafiltration system worldwide (Delgrange et al. 2000). Virus removal depends on the actual pore size and the molecular cut-off size of membranes. The MWCO (molecular weight cut off) indicates the molecular weight (MW) of those particles which still can pass the membrane efficiently. It was hypothesized that UF membranes can filter small virus, but actually, NF membranes only obtained 0.5 LRV removals of Qβ virus (Fiksdal and Leiknes 2006). A possible reason would be that the size distribution in UF membranes is big and existence of large pores may cause virus break through. Another common used filtration method is reverse osmosis (RO) membranes. This system can separate dissolved solutes using a semipermeable membrane. It does not need physical holes, which is the difference between RO membranes and other filtration membranes. RO membranes are

hydrophilic; they allow water to diffuse through the membranes easily. The set-up of RO membranes is simple and allows for large production capability (Wenten et al. 2002). But the limiting factor of RO membranes in virus removal is fouling and large transmembrane pressures. Increasing the number of removed virus increase the biological fouling. Other particles in water also increase the fouling (Pandey et al. 2012). This is a disadvantage of operating RO membranes.

Besides physical filtration, chemical and optical disinfection methods are also been used in water purification. Currently, chemical disinfection methods have been examined for their effectiveness on the removal of virus and bacteria (Sobsey et al. 2012). The treatments that had been considered are coagulation/chlorination, SODIS (solar UV radiation) and free chlorine. Coagulation/chlorination uses chloride as well as coagulation/flocculant. SODIS disinfection uses transparent polyethylene terephthalate bottles (PET or PETE) under solar UV light for several hours (Sobsey et al. 2012). All these methods proved to reduce bacteria (fecal coliforms and *E.coli*) at least 1 LRV. But they had trouble reducing virus (MS2-bacteriophages) over 2 LRV except for the coagulation/chlorination treatment. The SODIS disinfection technology is also limited to use in a lab due to the difficulties associated with the management of multiple PET or PETE bottles per day. For free chloride, 30% of users claimed that they had real detectable chloride levels by testing household-level water chlorination (Sobsey et al. 2012). There is still a need for improved water purification technique.

Right now, there is a great need of improvement of water disinfection methods for the next generation. Size-based filtering cannot easily filter small virus (Troccoli et al. 1998). The challenge of purifying water is removing small virus with a bio-friendly and easy to set-up disinfection technology that is not high in cost. In our studies, we are using the model virus porcine parvovirus (PPV). The diameter of PPV is 18-26 nm (Morrica et al. 2003). Mammalian parvoviruses, included PPV, are often used as model non-enveloped DNA viruses in viral removal experiments (Omar and Kempf 2002, Wickramasinghe et al. 2004). The structure of PPV and its protein have been reported (Simpson et al. 2002). PPV has multiple copies of the same protein on the surface of the virus. This provides multiple, identical binding sites on the virus surface and implies that

adsorption is likely a good method to remove the virus. Parvovirus are difficult to inactivate under various heat and pH environments (Kempf et al. 2007), demonstrating that they are difficult to chemical inactivate.

A series of experiments has shown that size-based filtration methods cannot filter or remove small virus easily. The Planova BioEX filter, used extensively as a virus removal membrane in the biotherapeutic industry, has the ability to remove virus greater than 40 nm (Kempf et al. 2007). However, smaller virus exists. PPV was only able to be removed after a series of filtration applications by only 2.6 LRV (Morrica et al. 2003). This creates a challenge for the filtration of small virus.

Studies demonstrated that positively charged surfaces can absorb virus. For negatively charged virus, they have been shown to bind to anion exchange absorbers, therefore effectively removing the virus (Riordan et al. 2009). Mark Etzel and his groups also tried adsorbing virus that has slightly acidic isoelectric points by changing the concentration of the buffer solution. They found that the buffer salt solution in the concentration range of 50-150 mM can adsorb the most virus. Anion exchange membranes with four chemical ligands (agmatine, tris-2-amineethyl amine, polyhexamethylene biguanide, and polyethyleneimine) performed better than membrane with quaternized amine (Q) ligands absorber (Riordan et al. 2009). Peptide ligands (WRW and KYY) have shown to be capable of capturing PPV. Virus can be removed up to 9 column volumes, where a column volume is the elution of liquid at the same volume as the packed column (Heldt et al. 2008). The peptides have one positively charged amino acid and two hydrophobic, benzyl-based amino acids (Heldt et al. 2008). It is possible to use these peptides in a water purification system.

It is hypothesized that PPV can be absorbed to any positively charged surface, including chitosan nanofibers. Chitosan is positively charged at a pH less than its pKa (6.4) (Inmaculada et al. 2009) due to the protonation of its amine groups. Various studies have shown that chitosan can react with negative charged solution like NaOH and ethanol (Inmaculada et al. 2009). NH_2 will transfer to NH_3^+ at a pH below its pKa; NH_3^+ can react with OH and COOH groups (Inmaculada et al. 2009).

Cation and anion membranes have shown an ability to remove Aedes aegypti densonucleosis virus, a non-enveloped virus, up to 2 LRV. By changing the pH of the solution above and below the pI of the virus, anion and cation exchange membranes can adsorb virus, respectively (Wickramasinghe et al. 2006). Increasing the size of the adsorbed species allows fewer particles to be removed by the membranes per constant membrane area. Because of the number of larger particles capable of binding to the surface area is less than the number of smaller particle in constant surface area. It is hypothesized that the mechanism for adsorbing both virus and proteins is similar, but the absorption capacity is different. It was hypothesized that the pore size and the need for multiple layers is critical for virus removal applications (Wickramasinghe et al. 2006).

It has been shown that ultra-fine nanofibers have the ability to absorb virus and remove bacteria by size exclusion. Electrospun nylon nanofibers have been shown to remove bacteria by size exclusion. The nanofibers can obtain a 8.6 LRV for *A.Laidlamii* and a 9 LRV for *B.Diminute*, compared to a 9 LRV produced by two commercial microfilter, Durapore VV and Express SHR. The pore size of the commercial filters is 0.2 μm. The pore size of the nylon nanofiber filter was not given (Kozlov et al. 2012). The nylon nanofibers were able to remove bacteria at the same LRV level as commercial membranes with reduced fouling and decreased transmembrane pressure. This demonstrated that nanofibers can improve membrane performance while maintaining a high bacteria LRV. Besides nylon, electrospun polyacrylonitrile (PAN) nanofibers have the ability to adsorb virus and sieve bacteria. The pore size of electrospun PAN was found to be 0.3 μm. When cellulose was infused into the PAN fibers, the pore size was restricted to 0.22 μm. The cellulose was added for pore size reduction. Electrospun PAN with cellulose was able to obtain a 6.0 LRV for *E.coli* and a 4.0 LRV for *B. diminuta*. The size of these bacterial are 0.5×2.0 μm and 0.3×0.9 μm, respectively (Ma et al. 2011). This proves that electrospun nanofibers have the strength and ability to filter bacteria by size exclusion. For MS2 bacteriophage virus, which has the dimensions of 27 ×32 nm, which is smaller than the pore size of electrospun nanofibers, electrospun PAN infused with cellulose can adsorb 2 LRV and the PAN nanofibers do not adsorb any virus when the cellulose is not present (Ma et al. 2011). They achieve much higher virus removal, comparing to 1.0 LRV of commercial negatively charged microfilter (Milipore,

GS9035). It is interesting that the negatively charged cellulose would enhance virus removal. However, the addition of positively charged polyethylenimine (PEI) increased virus removal to 4.0 LRV, as would be expected. The surface area is very high, 600 m^2 g^{-1}, which is higher than commercial microfilters. It is concluded that nanofibers with a higher surface area can adsorb more virus compared to standard microfilter. The pressure drop is also much less for nanofibers that commercial filters, creating a system that can remove virus with a low pressure drop (Ma et al. 2011).

Since most viruses are negatively charged due to the carboxyl and phosphate groups on their surface, it is hypothesized that positively charged nanofibers can adsorb virus and obtain higher LRV. After modifying electrospun PAN nanofiber with di-amine group, electrospun PAN nanofibers are positively charged in acid solution. Electrospun PAN had an average fiber diameter of 200 nm. Polyethylene terephthalate (PET) was used as a support to increase the strength and thermal resistivity of the nanofibers. Positively charged PAN was able to achieve a 4 LRV of MS2 bacteriophage virus, compared to a 2 LRV of unmodified, and negatively charged PAN nanofibers (Sato et al. 2011). It was conclude that positively charged nanofibers can use electrostatic force to adsorb virus. It is likely that the negatively charged nanofibers remove virus with a different mechanism as compared to the positively charged nanofibers. Similar result can be found with positively charged alumina nanofiber filters. Alumina nanofibers remove about 2 LRV of the MS2 bacteriophage (Li et al. 2009). To further prove the electrostatic attraction mechanism, alumina nanofiber samples were contacted with the same concentration of virus for different times. The number of plague-forming units (PFUs) decreased from 6×10^6 to 2×10^6 after 3 minutes and $< 1 \times 10^5$ PFU was detected after 10 minutes (Li et al. 2009). To remove virus with an adsorption filter, the filter must either have a high surface area or long contacts times. One method to increase the contact time is to have multiple filtration steps in series. For this reason, nanofibers are advantageous for virus removal due to their large surface area to volume ratios.

It is well documented that nanofibers, and in particular, chitosan nanofibers, can remove metals, chemicals and bacteria from water (Guibal et al. 2006). With these desirable properties, we would like to use chitosan to remove virus from drinking water. After a review of physical filtration, chemical disinfection, and nanofiber adsorption

12

methods, it appears that nanofiber adsorption is the best way to remove viruses while have low pressure drops and high water fluxes. However, there is still a need for improved surface chemistry to improve and analyze the adsorption of viruses to nanofibers. For this reason, we have chosen to electrospin nanofibers of chitosan to better understand the adsorption of viruses to fibers that are only one order of magnitude larger than the virus itself.

2.3   Electrospinning

One of the recent technologies for the production of nanofibers is electrospinning. Electrospinning can produce fibers with a diameter ranging from micrometer to nanometer. Wet-spinning can only produce fine-fibers (10 to 40 micrometers). The unique characteristic of electrospinning is that it can provide an easy and controlled method to produce nanofibers. Nanofibers are desired because they have a large surface area to volume ratio. High surface area provides more area to bind virus and can achieve higher virus removal and larger membrane capacities (Ma et al. 2011). This ratio can be as high as 103 times typical commercial microfilters (Huang et al. 2003). Nanofibers can also provide flexibility in their surface functionalities, and high tensile strength (Huang et al. 2003). All these benefits made nanofibers an excellent choice for biological application.

Electrospinning equipment contains a high-voltage power supply that pulls a viscous polymer solution to a rotating drum collector, while a syringe pump pushes the solution through the needle. A schematic of the system is found in Fig. 2.2.
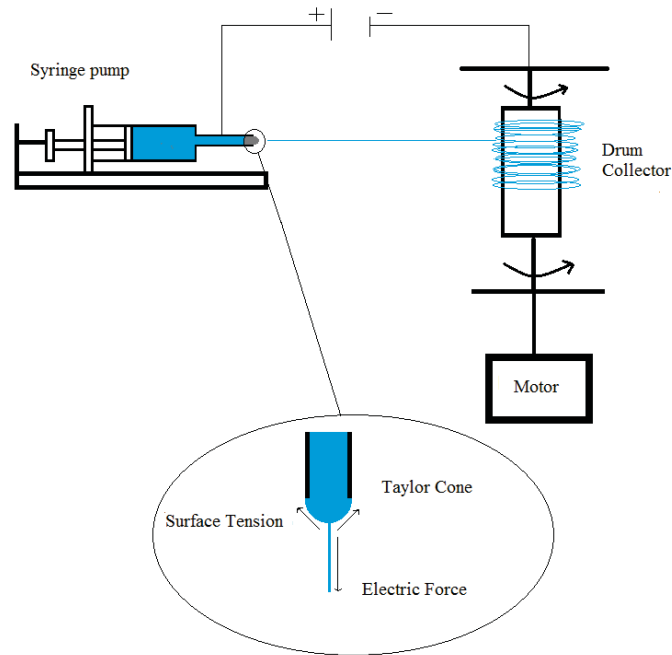
Figure 2.2 A laboratory setup for an electrospinning experiment (Geng et al. 2005)

The high voltage supply typically produces voltages between 1-20 kV. This high voltage introduces free charges to the solution inside of the syringe. When the electric force increases to the point where it can surmount the surface tension of the polymer solution, the charged solution is pulled to the opposite polarity drum collector. A pendant hemispherical droplet of polymer solution will form at the tip of the needle, looking like a cone from the needle to the collector, which is called a Taylor cone (Taylor 1969). When the polymer solution that is removed from the syringe by the electrical force is replaced by the addition of polymer solution from the syringe pump, then continuous fibers are formed. The polymer solution will dry and evaporate while the solution accelerates towards the collector in the electric field, forming dry nanofibers (Homayoni et al. 2009).

2.3.1 Electrospinning process Parameters

Electrospinning process parameter and the physical properties of the polymer solution can affect the fiber formation process. The applied voltage facilitates the charge

14

transport from the needle tip to the drum collector. Deitzel et al. has studied the instability modes of selecting polymer systems (Deitzel et al. 2001). They reported that increasing the applied voltage can change the mode of the jet of the electrospinning process, therefore changing the diameter of the fibers and the pore size of the nanofiber filter. Under low voltage, the fiber jets are produced at the bottom of the droplet. The jets initiate at the tip of needle when the voltage is increased (> 7 kV for a PEO polymer system) (Deitzel et al. 2001). When electrospinning a PEO/water solution, the morphology of the fibers was affected by the voltage. We prefer a bead-free morphology because the beads decrease the surface area and would reduce the filtration ability of the nanofibers. A study of the relation between voltage and fiber diameter of polystyrene (PS) demonstrated that increasing the voltage from 5 kV to 12 kV at the same distance decreased the fiber diameter from 20 μm to 10μm (Megelski et al. 2002).

The distance between the needle and the collector determine the evaporation time and the accumulation rate and therefore affects the diameter of the polymer fibers. It had been found that a shorter distance between the needle and the collector can spin wet fibers with beads, regardless of the polymer concentration. It also can change the morphology of SLPF (silk-like polymer with fibronectin) fibers from round to flat (Buchko et al. 1999). This shows that the distance between the needle and the collector influences the morphology of the fibers. It has also been shown that when a polymer solution is in highly volatile organic solvents, it needs less distance than aqueous polymer solutions (Buchko et al. 1999). Both voltage and distance played a role in fiber morphology, as well as the ratio of voltage to the distance.

Flow rate of the polymer solution can influence both the fiber size and the shape. It has been shown that only the consistent replacement of the polymer solution that is withdrawn into nanofibers can maintain the shape of the Taylor cone at the tip of needle (Taylor 1969). Megelski et al. reported that for a polystyrene/tetrahydrofuran electrospinning system that high flow rate will increase the number of beads because there is not enough time to dry the fiber before it reached the collector (Megelski et al. 2002). This incomplete drying process caused the formation of ribbon-like fibers (fibers with lots of beads). Overall, they found that the higher the polymer flow rate, an increase

in the fiber diameter can be found up to the point that bead formation begins (Megelski et al. 2002).

2.4 Chitosan

Chitosan is a natural chemical and biologically compatible material (Inmaculada et al. 2009). Chitosan is the deacetylated product of chitin. The structure of chitosan and chitin can be found in Fig 2.3.
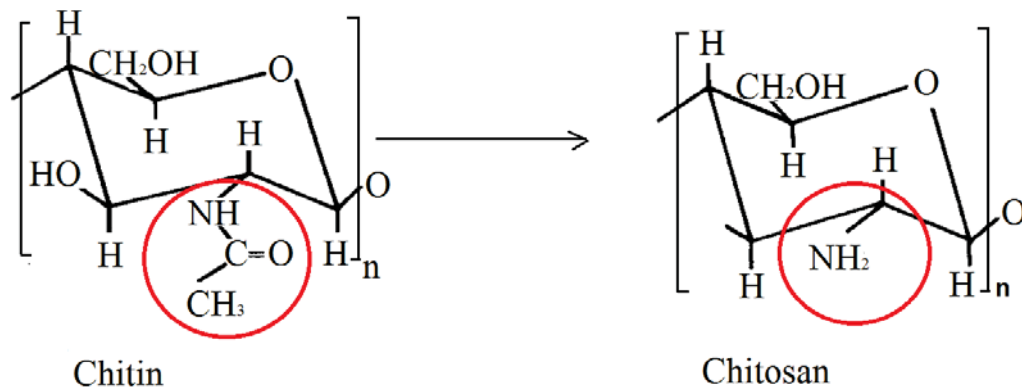
Figure 2.3 The Structure of chitin and chitosan

Chitosan-based polysaccharide hydrogels are biocompatible polymers that have excellent properties for future biomaterials. The DD changes the degree of crystallinity. Crystallinity represents the ability to form structure in the solid state (Areias et al. 2012). The large number of acetyl groups existing in chitin and chitosan also control the degree of biodegradability, with deacetylated chitosan being less biodegradable than chitin (Ignatious et al. 2000).

The cytotoxicity of chitosan molecules and nanoparticles has been studied. It has been demonstrated that the MW of the chitosan polymer solution and the DD can affect cytotoxicity. If the rate of the degradation process is very quick, the whole process will produce large amounts of amine groups and induce an inflammatory response. Different amounts of DD can also produce a different response. High DD produces an inflammatory response, whereas a low DD produces a minimal response (Kurita et al. 2000). Kofuji et al. studied how the MW and viscosity of chitosan can affect the

enzymatic degradation of the chitosan. The decrease of viscosity under the same MW and decrease of DD under the same MW decreased the degradation (Kofuji et al. 2005). The relation between the DD and the toxicity has been examined. A DD >35% can represent lower toxicity. It also demonstrated that the molecular weight of chitosan did not affect toxicity (Schippere al. 1996). Chitosan (which has a higher DD than chitin) was less toxic than chitin in *in vitro* experiment against different kind of cells, ranging from myocardial, endothelial and epithelial cells (Chatelet et al. 2001). Since chitosan is positively charged, the relationship between charge and interaction between chitosan and the cells was examined. The increase of amine groups will increase the charge of the chitosan and therefore cause a stronger interaction between chitosan and cells. But different cells showed various reactions with chitosan. But no matter what kind of cell it is, the degree of DD can influence the interaction with cells with respect to adhesion and proliferation. Increasing the DD will reduce cell proliferation. The impact on cell adhesion is less straightforward. It depends on both the DD and cell type (Chatelet et al. 2001).

Chitosan is known for its antimicrobial activity. It is generally accepted that the amine group of chitosan can react with the anionic groups on the bacteria cell surface and this interaction brings extensive change to the cell surface and the cell permeability (Sudardshan et al. 1992, Fang et al. 1994, Hwang et al. 1999). Cell permeability causes leakage of intracellular substances and often leads to cell death. This mechanism has been demonstrated with electron microscopy (Helander et al. 2001). Adding acid can increase the positive charge of the chitosan by moving further from the pKa of chitosan, and increasing the ability to cause cell leakage (Helander et al. 2001).

A study about the relationship between the molecular weight of chitosan and its antimicrobial activity showed that chitosan had the ability to inhibit the growth of *Candida albicans, Candida krusei* and *Candida glabrata* (Seyfarth et al. 2008). However, the antibacterial activity of the chitosan monomer, D-glucosamine hydrochloride, against bacteria is almost zero. This shows that the MW influences the antimicrobial activity (Seyfarth et al. 2008). Others have examined the influence of polymerization of chitosan on antifungal activity (Kendra and Hadwiger 1984). They found that monomer and dimer of chitosan cannot produce any antifungal activity at the minimum concentration (0.5 wt%). The heptamer had the best antifungal activity, for those tested, which proved that

17

antifungal activity increased with the increasing MW of chitosan (Kendra and Hadwiger 1984). Shimojoh et al. had a similar conclusion when studying the antibacterial properties of chitosan. Chitosan with a different MW but at the same concentration and the same DD were studied. Again, against *E.coli*, they found that bactericidal activities increased with the increasing of MW (Shimojoh et al. 1996). For others, the conclusion is reversed. It is suggested that the microorganisms targeted also influences the bactericidal activities (Kurita et al. 2000). The microorganisms target and MW can influence the antifungal and antibacterial activity of chitosan. Comparing the antibacterial activity of chitosan with MW in the range of 10,000–170,000, chitosan with MW 30,000 has the highest antibacterial activity (Hwang et al. 1999). Jeon et al. showed that MW more than 10,000 can show the better antimicrobial activity (Jeon et al. 2001). Generally, antimicrobial activity will increase with the increase of the MW. When the MW is high enough, according to experimental result, antimicrobial activity will decrease with the increasing of MW above some critical point, making it difficult to define an optimized MW and DD.

Liu et al. found that positively charged chitosan can interact with the cellular DNA of some bacteria. This interaction can reduce the translation of DNA and the synthesis of protein (Liu et al. 2001). The authors hypothesized that the amine groups may reduce the number of *E.coli*; this is the main reason to explain that O-CM-chitosan had the best antibacterial activity, following by chitosan and *N, O*-carboxymethylated chitosan. The structure of these polymers can be found in Fig 2.4. O-CM-chitosan is a product of substitution of hydroxyl groups with carboxymethyl groups. *N, O*-carboxymethylated chitosan is produced by replacing the amine groups and hydroxyl groups in chitosan with carboxymethyl groups (Liu et al. 2001). They also found that the antibacterial ability of chitosan increased with an increasing MW and DD. Under various pH conditions, the antibacterial ability of chitosan had been examined. Below pH at 6.4 (chitosan's pKa is 6.4), chitosan had the best antibacterial due to the large number existence of charged $-NH_3^+$ groups (Liu et al. 2001). The antibacterial activity of chitosan was enhanced with increasing MW from 5000 to 9.16×10^4, and then descended with increasing MW from 9.16×10^4 to 1.08×10^6. Too high MW inhibited the diffusion of functional groups due to the high viscosity of the solution (Liu et al. 2001). The DD is also a factor that affects

18

the antimicrobial activity, by increasing the number of amine groups on the polymer, the antibacterial effect is increased (Liu et al. 2001, Tsai and Su 1999). Chitosan can dissolve better in water with lower DD (Liu et al. 2001). There will be more chance for chitosan to interact with negatively charged bacteria and cell.
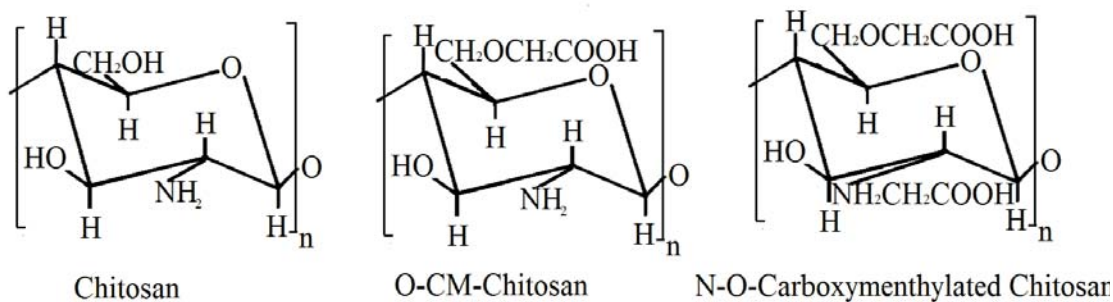

Figure 2.4 The structure of chitosan and O-CM-Chitosan and N-O-Carboxymethylated chitosan

Temperature of incubating 150 ppm chitosan solutions can influence the antimicrobial activity of chitosan against *E. coli*. It was tested at four temperatures, $4\,^{\circ}C$, $15^{\circ}C$, $25^{\circ}C$, and $37^{\circ}C$. At a temperature of $25^{\circ}C$ and $37^{\circ}C$, chitosan can kill all the cells within 5 and 1 hours, respectively. Higher temperatures can kill the cells in a shorter time (Tsai and Su 1999). Overall, chitosan with higher MW produced higher antimicrobial ability and chitosan with higher DD also increased antimicrobial ability, along with higher temperature. The pH of the solution needs to be below the pKa of chitosan.

2.5 Electrospinning Chitosan

Many researches had studied the preparation of chitosan to be electrospun (Li et al. 2006, Geng et al. 2005, Ohkawa et al. 2004, Homayoni et al. 2004, Duan et al. 2006). Chitosan is not soluble in water due to the rigid D-glucosamine structure, easily formed crystals and the likelihood to form hydrogen bonds. Decreasing the MW and crystallinity can increase chitosan's solubility (Li et al. 2006). It was found that one difficulty while electrospinning chitosan is the high solution viscosities due to the polyelectrolyte effect. Polyelectrolyte effect is caused by the repeating electrolyte groups in the polymer. The electrolyte groups increase their hydrogen bonding as the concentration increases. These

groups dissociate in aqueous solutions, and the polymers are charged. Another reason for the high viscosity is the fast coagulation rate. One method to electorspin pure chitosan at a 7 wt% concentration is to solubilize the polymer in 90% acetic acid (Geng et al. 2005). Another method to increase the solubility and decrease the viscosity of chitosan is to add sodium acetate, which decreases chitosan's entanglement and crystallinity (Kulish et al.2006). Another method to improve the electrospinning ability of chitosan is to use additives (Ohkawa et al. 2004, Homayoni et al. 2004, Duan et al. 2006). Additives can change the diameter of electrospun fibers, diameter of electrospun chitosan/PVA fibers increased from 20 nm with 75% PVA to 100nm with 89% of PVA (Li et al. 2006). A series of common additives can be found in Table 2.1

Electrospun 2 wt% chitosan/PEO solution in 10% acetic acid obtained fibers with a diameter ranging from 40-290 nm. But fibers diameter within 200-250 nm were the only ones that were defect-free (Homayoni et al. 2004). When studied closely, it was found that PEO and chitosan are separated in electrospun fibers (Bhattarai et al. 2005). Larger fibers are PEO and the smaller ones are chitosan. It showed that there is an inconsistent flow during the electrospinning process. Research found that adding Triton X-100™ to chitosan/PEO blend solution can decrease the distribution of the size of fibers. With nonionic surfactant as additives, chitosan can be spun at a higher concentration (Bhattarai et al. 2005).

Research about electrospinning 1 wt% chitosan/PEO water solution has reported that fibers with a 300 nm diameter can be produced; PEO was 5 wt% of chitosan. By testing the cellular viability of chitosan nanofibers formed via electrospinning, it has been shown that chondrocyte cells can adhere better in the existence of electrospun fibers, comparing to pure cells (Subramanian and Lin 2005). In a previous report, PEO used as additives to chitosan in electrospinning because PEO had good biocompatibility, low toxicity and can be electrospun. Chitosan/PEO fibers successfully electrospun defect-free fibers within the diameter range of 80-300nm (Homayoni et al. 2004, Duan et al. 2006). They demonstrated that the PEO additive increases cellular growth and wound healing.

Table 2.1
Electrospun chitosan with various additives

Polymer	DD	Average Diameter (nm)	Concentration(wt)	Reference
Chitosan/PVA	90	99±21	4 -8 wt%	Zhang et al. 2005
Chitosan/collagen	7	436-690	6 -12 wt%	Chen et al. 2010
Chitosan/PCL	-	190±20	8 wt%	Prabhakaran et al. 2008
Chitosan/nylon-6	85	80-310	6 wt%	Zhang et al. 2009
Chitosan/PVA-PLGA	90	275±175	5 wt%	Duan et al. 2006
Chitosan/SF	86	180-790	3.6-12 wt %	Park et al. 2004
Chitosan/HAp/UHMWPEO	85	215±25	12 wt%	Zhang et al. 2008

Solution concentration will affect viscosity and surface tension of the solution, in turn affecting the spinning conditions and morphology of the fibers (Deitzel et al. 2001). If the concentration is too high, then the high viscosity prohibits fiber formation because it needs much more force than the electrostatic force can provide. Higher concentrations (12 wt%) reduce the number of beads compared to lower concentration (7 wt%) (Ki et al. 2005), so a small window is present where the viscosity is high enough to produce defect-free fibers without being so high as to prevent fiber

formation. Several groups have reported that below a certain concentration, polymers solution cannot be electrospun; like PEO (5 wt%) (Deitzel et al. 2001) and PAN (7 wt%) (Fridrikh et al. 2003).

The jet formation is highly depending on the charge of the solution. Most polymer solutions are conductive, leading to higher concentration polymer solutions having a higher charge. This increases the solutions ability to form a jet at the same voltage, and therefore forms a system where the solution can spin more easily. Studies have shown that changing the conductivity of a PDLA (poly (D-lactide)) system will affect the diameter of the fibers formed by electrospinning. It showed that increasing the charge of the solution facilitates the creation of bead-free fibers (Zong et al. 2002). A higher conductivity can reduce the number of the beads (Buchko et al. 1999).

Quaternary ammonium compounds have antimicrobial ability (Worley and Sun 1996). Introducing quaternary amine group into chitosan may increase the biocidal ability by increasing the positive charge of the polymer and the water solubility. Studies showed that quaternized *N*-alkyl chitosan had antibacterial activities against *E. coli*. The structure of quaternized *N*-alkyl chitosan can be found in Fig 2.4. The results showed that MW affects antibacterial activities of quaternized *N*-alkyl chitosan against *E. coli*; higher MW produced higher antibacterial activities. Two solvent had been compared, for antibacterial activities, acetic acid solvent is better than that in water. Higher concentration of acetic acid produced higher antibacterial activities. Quaternized *N*-alkyl chitosan (minimum inhibitory concentration (MIC) 0.25 mg/ml) had higher antibacterial activities as compared to chitosan (MIC is 2.5 mg/ml) (Jia et al 2001).
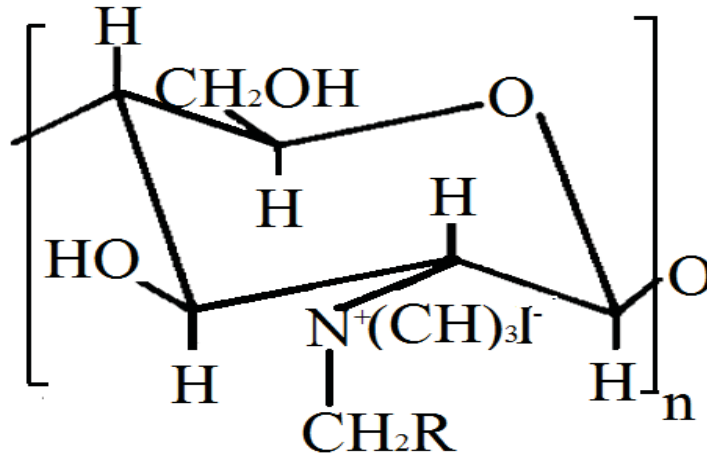
Figure 2.5 The structure of quaternized N-alkyl chitosan (Jia et al. 2001)

Now, it is known that quaternized chitosan derivatives have higher antibacterial activities than chitosan. We hypothesized that quaternized chitosan derivatives can also remove virus effectively due to the increase of the positive charge as compared to chitosan. In order to apply quaternized chitosan derivatives as a water purification system, we electrospun quaternized chitosan derivatives to produce nanofibers. These nanofibers were studied for their fiber morphology and virus removing ability.

3   Materials and Methods

3.1   Materials

Chitosan of 310,000 molecular weight and 75-85% deacetylated was purchased from Sigma (St.Louis, MO). Additives to enhance electrospinning included polyvinyl alcohol (PVA) (MW = 89,000-98,000, degree of hydrolysis 99%), polyethylene oxide (PEO) (MW = 900,000), sodium dodecyl sulfate (SDS) (for molecular biology, $\geq$ 98.5%) were all purchased from Sigma (St. Louis, MO). Graphene was made by Xu Xiang in Dr. Heiden's lab. Silver nitrate (ReagentPlus®, $\geq$ 99.0%) and potassium chromate (ACS reagent, $\geq$ 99.0%) for chloride titration were purchased from Sigma (St. Louis, MO). Whatman Quantitative Filter Paper Circles (Clifton, NJ), Grade 1, 55mm and 10 mm diameter were used as a nanofibers support. Syringe (3 mL Luer-Lok Syringe 23g x 1" PrecisionGlide Intramuscular Needle) was purchased from Fisher Scientific (Pittsburgh, PA).Fluorescent microspheres (1.06 µm diameter and 4.6 µm diameter) with an excitation and emission wavelengths of 480 and 520 nm, were purchased from Bangs Laboratories INC (Fishers, IN) for pore size determination.

To make N-[(2-hydroxy-3-trimethylammonium) propyl] chitosan chloride (HTCC), glycidyl-trimethylammonium chloride (GTMAC) (technical grade, $\geq$ 90%) was purchased from Sigma (St. Louis, MO). Dialysis Tubing (Fisher brand regenerated cellulose dialysis tubing - 3500 Dalton MWCO; diameter: 12.1 mm) was purchased from Fisher Scientific (Pittsburgh, PA).   All cell culture solutions were purchased from Invitrogen (Carlsbad, CA), unless stated otherwise. For virus titration, MTT reagent, thiazolyl blue tetrazolium bromide (powder, BioReagent, $\geq$ 97.5%) was purchased from Sigma (St. Louis, MO). All water was purified to >18 MΩ by a Nanopure system (Fisher Scientific, Pittsburgh, PA

3.2   Methods

3.2.1 Electrospinning chitosan solution

In the literature review section, the electrospinning equipment has been introduced. The electrospinning experiments were done in a home-made apparatus. A total of 2 ml of chitosan/PEO in 90% acetic acid was made and stirred in a sonicator (Fisher Scientific Mechanical Ultrasonic Cleaners, Pittsburgh, PA) for 30 minutes. Then the solution was transferred to a 3 ml syringe. The syringe was attached to a syringe pump (Braintree Scientific INC, Braintree, MA) and the needle was connected to the high voltage supply (Glassman high voltage, INC, High Bridge, NJ), while the ground was attached to the rotating drum collector that was run by a pump (ElectroCraft TorquePower™, Ipolis, OH). The rotation speed was 2000 rpm. Filter paper was taped on the drum collector that was covered with aluminum foil to collect the fibers. The distance between the tip of needle and the drum collector was 10 cm. The feed rate was controlled in the range of 5 ml/h-10 ml/h. We worked in the voltage range from 10 kV to 20 kV.

3.2.2 Characterization of chitosan nanofibers

In order to establish the relationship between fiber diameters and pore size, we filtered fluorescent polymer beads with various chitosan nanofibers. First, we performed a standard curve of known polymer concentration versus fluorescence in the range of 0 to 2.5 ppm. We prepared a 2 ppm fluorescent polymer solution and filtered 1 ml of the fluorescent polymer solution with various chitosan nanofibers. The fluorescence was read of fluorescent polymer solution before and after the filtration on a Synergy Mx Monochromator-Based Multi-Mode Microplate Reader (Winooski, VT). The excitation and emission wavelengths were 480 and 520 nm, respectively.

SEM micrographs were obtained using a Hitachi S-4700 FE-SEM Cold field emission, high resolution scanning electron microscope (Tustin, California) at an accelerating voltage of 5 kV and magnification of 1,000× to 80, 000×. Due to the non-conductive nature of the nanofibers, the nanofibers were coated with gold prior to SEM imaging. A 5 nm layer of gold was applied to the surface of nanofibers using a sputter coater (Hummer Sputtering System, Union City, CA) at a rate of 0.1 nm/min. After

coating the nanofibers with gold to a thickness of 5 nm, a 1 cm^2 section was cut from the middle of the sample for SEM imaging. Each SEM image is represented at 4 images.

Fiber diameters were measured with Image J (NIH). This was done by calibrating the scale bar and then measuring the diameter of 30 single fibers.

3.2.3 Cell propagation, virus titration and virus removal.

Porcine parvovirus (PPV) strains NADL-2 and porcine kidney (PK-13) cells were a gift from Dr. Ruben Carbonell, North Carolina State University. The cells were propagated and titrated as described previously (Heldt et al. 2006). Briefly, the cells were removed from the flask with 0.25 % trypsin and transferred to a 15 ml tube. A pellet was formed by centrifugation and the cells were split at a ratio of 1:5 every 3-4 days.

For virus titration (Heldt et al. 2006), cells were seeded at a concentration of 8×10^3 cells/well in 100 µl into a 96-well cell culture plate. After 1 day incubation, the cells were infected with PPV samples by adding 25 µl/well of PPV and serially diluting 1:5 across the plate. Titration was performed in quadruplicate. After 5 days, 10 µl/well of 5 mg/ml MTT salt in PBS was added to the 96-well plates and incubation at 37 °C. After 4 h, 100 µl/well of the solubilization buffer (10% SDS in DI water contain 0.01M HCl) was added. The next day, the absorbance of the plates was read on a Synergy Mx Monochromator-Based Multi-Mode Microplate Reader (Winooski, VT) at 550 nm. The virus titer was calculated by determining the dilution of virus that reduces the cell density to 50% of the control cells and this dilution was designated the MTT titer.

PPV was contacted with electrospun nanofibers and the PPV concentration was tested by titration with the MTT assay before and after contact with the nanofibers. A 500 µl PPV solution containing 6 logs (MTT/ml) in PBS (phosphate-buffered saline, KH_2PO_4 (15.44 mM), NaCl (1551.72 mM), Na_2HPO_4-$7H_2O$ (29.07 mM), pH 7.2) was placed into each tube. By changing the concentration and ratio of KH_2PO_4 and Na_2HPO_4-$7H_2O$, we can control the pH. One piece of 1.5 cm square, grade 1 filter paper with chitosan

nanofibers was placed into each tube containing virus. The blank was the tube with only virus. Tubes were rotated for 5 hours on a Roto-Shake Genie (Scientific Industries, Bohemia, New York).

3.2.4 Prepare and electorspun HTCC

HTCC was produced in a similar manner as has been shown before (Alipour et al.2009). Chitosan (1.6 g) was dispersed in a round-bottom beaker, then GTMAC (0.04 mol, 6.06 g) and 50 ml DI-water were added. The blend solution was stirred for one day, maintaining the temperature at 80 °C with an oil bath. The unreacted chitosan was filtered with a Buchner funnels by grade 4 filter paper. The solution was concentrated under vacuum (KNF LAB, Filtration Pump, Trenton, New Jersey). Dialysis tubing was used to dialyze the solution to remove any unreacted GTMAC for 24 hours in a water bath. The solution was again concentrated under vacuum. To achieve a higher yield of the quaternizing product, the solution was precipitated in acetone at 4 °C. The precipitate was dried in an oven (Fisher Scientific, Isotemp, Model 281A Vacuum Oven, Pittsburgh, PA) for 12 h at 60 °C. The chemical synthesis scheme of HTCC formation can be found in Fig 3.1

To prepare the HTCC solution for electrospinning, various additives were dissolved with HTCC at a total concentration of 10%, unless otherwise stated, in water. A sonicator (Fisher Scientific, FS20, Pittsburg, PA) was used to blend solution for 1 hour. HTCC blend solutions were electrospun similar to chitosan.
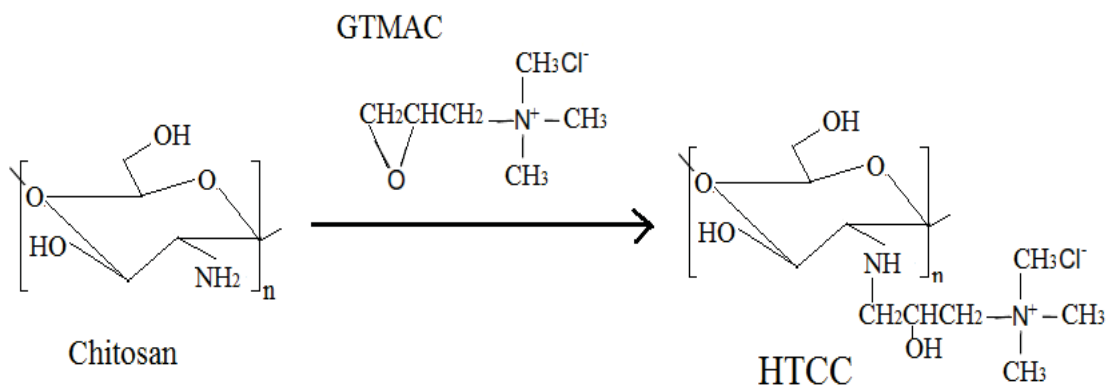
Figure 3.1 Synthesis of HTCC (Alipour et al. 2009).

3.2.5 Characterization of HTCC nanofibers

To measure the degree of quaternization (DQ) of HTCC, we used titration of chloride content at room temperature (Chang 2010). A 1 wt% silver nitrate solution was placed in a burette. A total of 25.00 ml of the 1 wt% HTCC solution was transferred to a 125 ml Erlenmeyer flask. Then, 5 ml of 1 wt% potassium chromate solution was added to the Erlenmeyer flask. The 1 wt% silver nitrate solution was added to the HTCC solution until the solution became orange-red color. The final titration point was recorded and the weight of HTCC was calculated. Degree of quaternization is calculated as described below:

a= initial mass of reacted chitosan × 80% (average value of DD)

b= unreacted mass of chitosan

c= weight of dry mass of HTCC after reaction

M_{u1}= unit molecular weight of chitosan

M_{u2}= unit molecular weight of HTCC

x=degree of quaternization

y=moles of Cl^{-1} (resulted from titration)

$$x=\frac{y}{\frac{(a-b)}{Mu1}} \tag{3.1}$$

$$y\times M_{u2}+\frac{(a-b)}{Mu1}(1-x)\times Mu1=c \tag{3.2}$$

FTIR spectra were measured using a Perkin Elmer FT-IR Spectrum One Spectrometer (Shelton, CT). HTCC was measured at 10mg/ml in water and chitosan was measured at 2mg/ml in 90% acetic acid using KBr pellets. NMR spectra were measured on an OXFORD NMR400. HTCC (10 mg/ml) was dissolved in D_2O/HCl (100/1 v/v), and chitosan (5 mg/ml) was dissolved in CF_3COOD for NMR analysis. Due to the likelihood of unreacted chitosan remaining in the HTCC, HCl was added to dissolve the chitosan in the HTCC. Conductivity of each additive–HTCC blend solution was measured with a conductivity meter (Fisher Scientific Accumet Basic AB30 Conductivity Meter, Pittsburgh, PA). Viscosities of the electrospinning solutions were measured with an SV-10 Vibro-viscometer (Malvern, United Kingdom). HTCC nanofibers were imaged with SEM with the same protocol as the chitosan nanofibers. Each SEM image is represented of two images.

In order to better understanding the adsorption mechanism of virus to HTCC nanofibers, the Langmuir isotherm equation (Eq. 3.3) was used to model the virus adsorption. The Langmuir model assumes that the surface only has monolayer adsorption, each adsorption site is equivalent and independent, and the adsorption is homogeneous (Sohn and Kim 2005). To determine the constants in the equation, K_d and q_m, which represent the equilibrium dissociation constant and the maximum binding capacity, respectively, the Langmuir equation is linearized, as shown in Eq. 3.4.

The original form of Langmuir model is the following:

$$q = \frac{q_{max}C}{K_d + C} \tag{3.3}$$

The linearized form of Langmuir model is the following:

$$\frac{C}{q} = \frac{K_d}{q_m} + \frac{C}{q_m} \tag{3.4}$$

C is the equilibrium concentration of virus in solution after adsorption onto the nanofibers in units of MTT/ml and q is the amount of virus bound to the nanofibers in units of MTT/μm^2 which is the amount of virus adsorbed per surface area of nanofiber available for adsorption. To calculate the surface area of the nanofiber, first the fiber density must be determined. The fiber density can be measured from the SEM images by

counting the number of fibers on each SEM image and dividing by the actual area of the image (Wang et al. 2009). The total surface area of nanofibers on one piece of filter paper is SA_t and is calculated by $SA_t = $ (fibers/ μm^2) × (area of filter paper) × (SA/fiber). SA is the surface area of a nanofiber. q is the (virus removed) × (volume of virus) / SAt in the units of MTT/ μm^2. Surface area of nanofibers is $SA = 2\pi \times r \times L$ (μm^2/ fiber). r is the radius of nanofibers and L is the length of the filter paper. Here we assume that each nanofiber runs the length of the filter paper.

4 Results and Discussion

4.1 Chitosan Nanofibers

We would like to produce polymer nanofibers that remove virus for water purification applications. The polymer nanofibers are produced by electrospinning, a process that applies an external electric force to a polymer solution to produce various ultra-fine polymer fibers. Chitosan is a promising biofriendly polymer for a lot of biological applications and is known to bind to virus (Davis et al. 2012). This work explores the fabrication of electrospun chitosan nanofibers and examines their ability to remove virus from solution.

Chitosan cannot dissolve in water; however, it can be dissolved in certain solvents, included acetic acid and ethanol (Rinaudo et al. 2006). In this work, we chose to use 90% aqueous acetic acid as the solvent for chitosan. Second, it is hard to electrospun pure chitosan solution due to its high viscosity. Chitosan has rigid d-glucosamine units (Rinaudo et al. 2006), and easily forms hydrogen bonds. Adding 10-20 wt% polyethylene oxide (PEO) of total polymer weight decreases the viscosity of blend solutions and also helps the solution to be electrospun. PEO can reduce the formation of chitosan's internal hydrogen bonds because PEO forms bond with chitosan. To optimize the creation of defect-free nanofibers, chitosan was electrospun at different voltages and concentrations to determine the best electrospinning conditions. The images of electrospun chitosan at various voltages can be found in Fig 4.1.

According to Fig 4.1, increasing the voltage of chitosan/ PEO (9:1) blend solution in 90% acetic acid from 12.5 kV to 20 kV can reduce the number of beads. The polymer solution is being pushed by the syringe faster than the electrical force can pull the polymer away from the needle tip at 15 kV and lower for this feed rate. This is shown by the presence of beads in the nanofibers. The voltage should be larger than 15kV for this concentration and feed rate of chitosan/PEO. We could like to produce defect-free

31

nanofibers; nanofibers with beads reduced the high surface area to volume ratio and therefore the removal efficiency will be reduced.
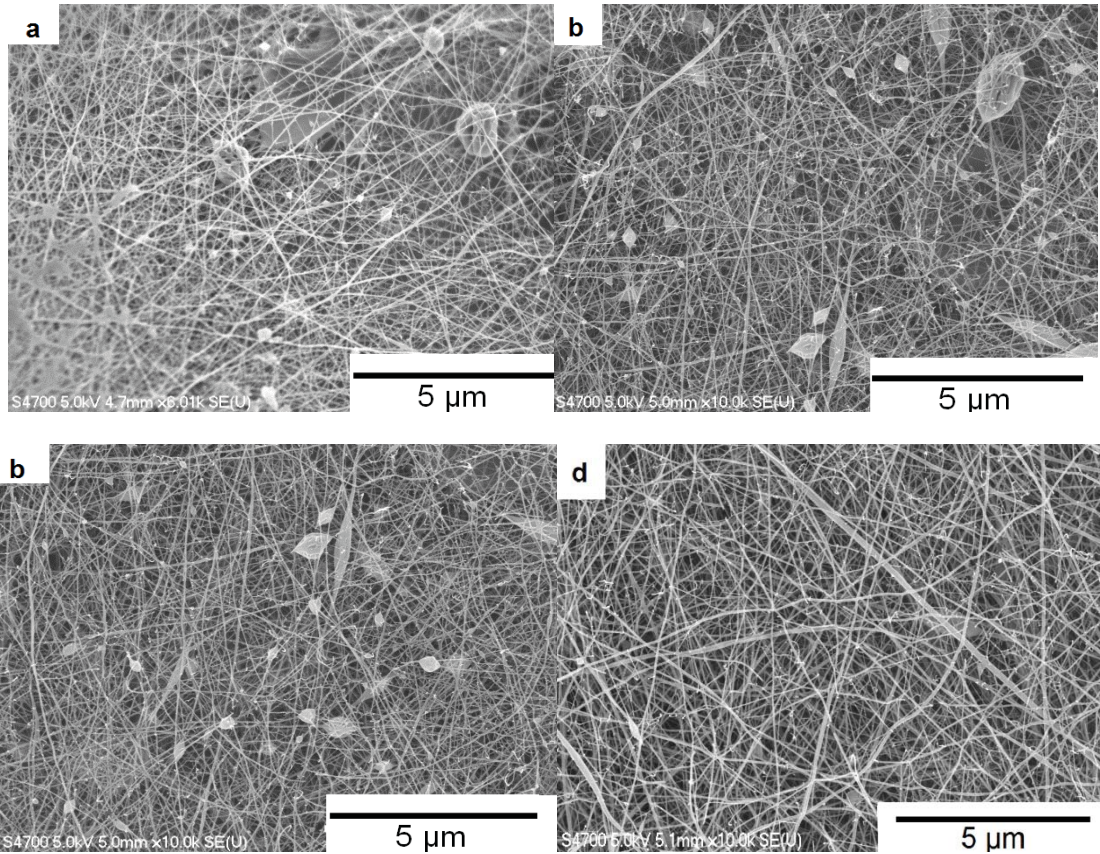

Figure 4.1 SEM micrographs of electrospun chitosan/PEO (In 90% acetic acid at different voltages. The mass ratio is 9:1, feed rate is 6 ml/h, concentration is 2.5 wt%, distance is 10 cm, and voltage for each sample is (a) 12.5 kV; (b) 15 kV; (c) 17.5 kV; (d) 20 kV.)

Since voltage at 20 kV created defect-free nanofibers, it was necessary to examine the influence of polymer concentration. We electrospun chitosan solutions from 1.25 – 2.5 wt% in 90% acetic acid and imaged them with SEM. The SEM images can be found in Fig 4.2. Increasing the concentration of chitosan, PEO (9:1) blend solutions, from 1.25 wt% to 2.5 wt%, we can see a reduction in the number of beads. Higher concentrations translated into higher viscosities; therefore the goal was to produce a polymer solution with a high viscosity. McKee et al. had a similar conclusion in previous experiment

(McKee et al. 2004). They electrospun linear and branched poly (ethylene terephthalate-co-ethylene isophthalate) (PET-co-PEI) copolymers with various concentrations. A minimum concentration of polymer was required for electrospinning, and then the concentration for producing defect-free and uniform fibers was two times larger than the minimum electrospinning concentration (McKee et al. 2004).
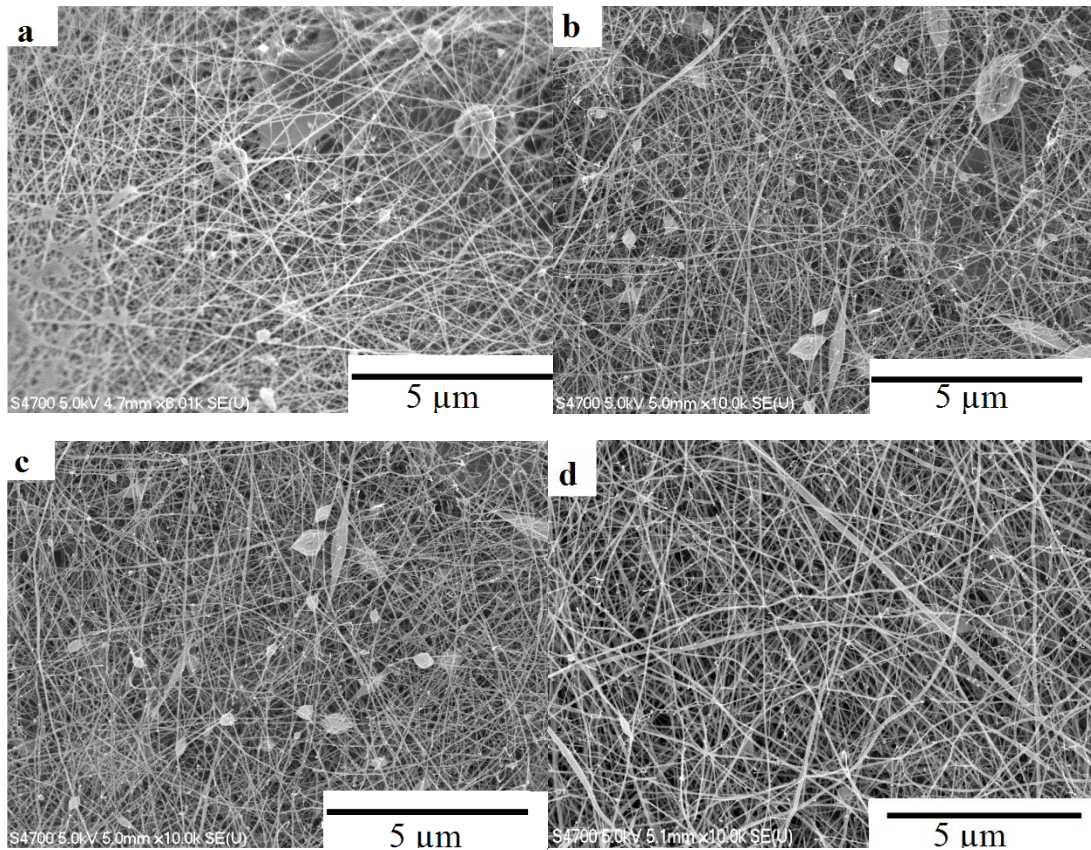

Figure 4.2 SEM micrographs of electrospun chitosan/PEO(In 90% acetic acid at different concentration, the mass ratio is 9, feed rate, 6 ml/h, distance is 10 cm and voltage density is 20 kV. The concentration for each sample is (a) 1.25 wt%; (b) 1.75 wt%; (c) 2 wt%; (d) 2.25 wt%.)

4.1.1 Chitosan Nanofiber Characterizations

Our goal was to create positively charged nanofibers that could be applied as a virus removal system. We preferred a high volume to surface area ratio, and therefore smaller diameter nanofibers, to produce a high virus binding surface. In order to acquire the relationship between the diameter of chitosan/PEO fibers and the electrospinning

conditions, a series of experiments were carried out using various voltages and feed rates of chitosan/ PEO (2.5 wt%) (9:1) blend in 90% acetic acid. A chitosan/ PEO (2.5 wt %) (9:1) blend was electrospun in a range of 15 to 20 kV and at feed rates in the range of 5.0 to 9.2 ml/h. Image J was used to calculate the average diameter of the nanofibers. The average diameters of the electrospun nanofibers at each voltage and feed rate are shown in Fig 4.3.
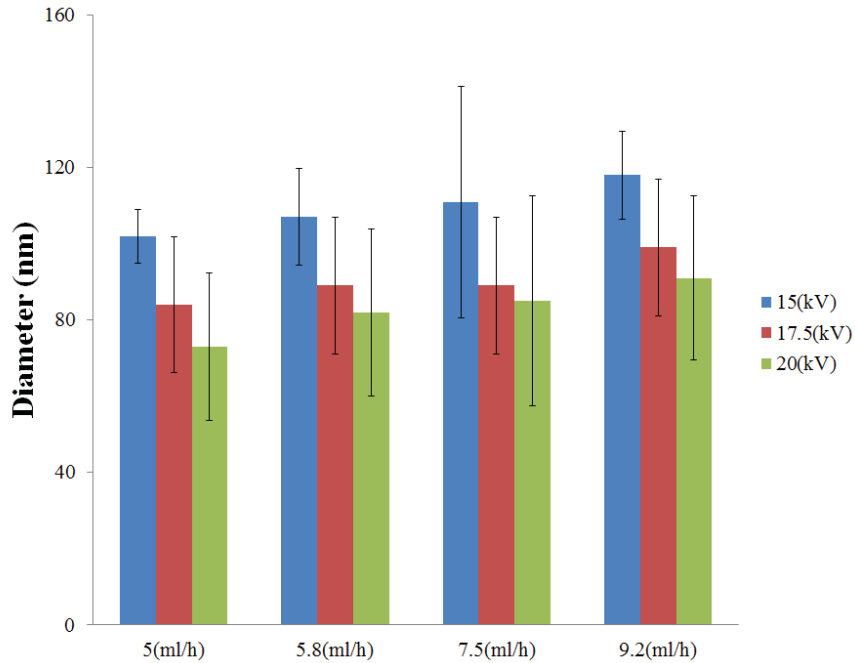

Figure 4.3 Relation between diameter and feed rate and voltage

The results show that the diameter of electrospun chitosan/PEO in 90% acetic acid fibers were in the range of 70–120 nm and could be precisely controlled. The diameters of chitosan/PEO in 90% acetic acid fibers decrease with increasing voltage at a constant feed rate and increase with increasing the voltage at a constant feed rate. In order to know if the data is significant to each other, we compared each column using the student t-test. Comparing within the same feed rate, all of the different voltages were statistically significant, with a p value of <0.05, except for the difference between 17.5 kV at 9.2 m/h and the other voltages at that feed rate. Within the same voltage, there is not a statistical difference between flow rates, to a p value of 0.05. This supports the conclusion that

increasing the voltage decreases the fiber diameter. Higher voltage means higher electrostatic force. As the electrostatic force overcomes the surface tension of the polymer blend, a jet is formed of polymer solution. As the electrostatic force increases even more, the jet is sharpened and creates thinner nanofibers (Deitzel et al. 2001). Increase of feed rate increases diameter, although not with a statistical difference. This may be due to more solution being ejected from the needle and evaporating during a constant time. Therefore an increase in the mass rate increases the fiber diameter.

With precise control over fiber diameter, we then wanted to understand the relationship between fiber diameters and pore size. To study pore size, we filtered fluorescent polymer beads of 1.06 and 4.6 μm diameter. A fluorescent bead solution at a concentration of 2 ppm was filtered with nanofibers of different diameters. The result of the removal of the fluorescent beads can be found in Fig 4.4.

We first developed a standard curve to understand the relationship between polymer bead concentration and fluorescence, and this linear curve can be found in Fig 4.4a. Based on this standard curve, we measured the concentration of beads before and after filtration with different diameter of chitosan/PEO nanofibers and calculated a percent removal. According to Fig 4.4b, the lowest removal was obtained by the smallest nanofibers. For 4.6 μm fluorescent polymer, the highest removal (65%) was obtained by the largest diameter (118 nm) of nanofibers; a similar result can be found in 1.06 μm fluorescent polymer. An increase in diameter of the nanofibers produced a higher bead removal. This demonstrates that as fiber diameter increases, the pore size of the nanofiber mat decreases. This is likely because the larger fibers take up more room on the filter and decrease the area remaining for open pores. Fig 4.4c proved that fluorescent beads were removed by the chitosan nanofibers. These results correspond to the pervious experiments. For electrospun PEO nanofibers, the diameter of fiber increased from 95 nm to 350 nm as the pore size decreased from 563 to 153 μm (Dotti et al. 2007).
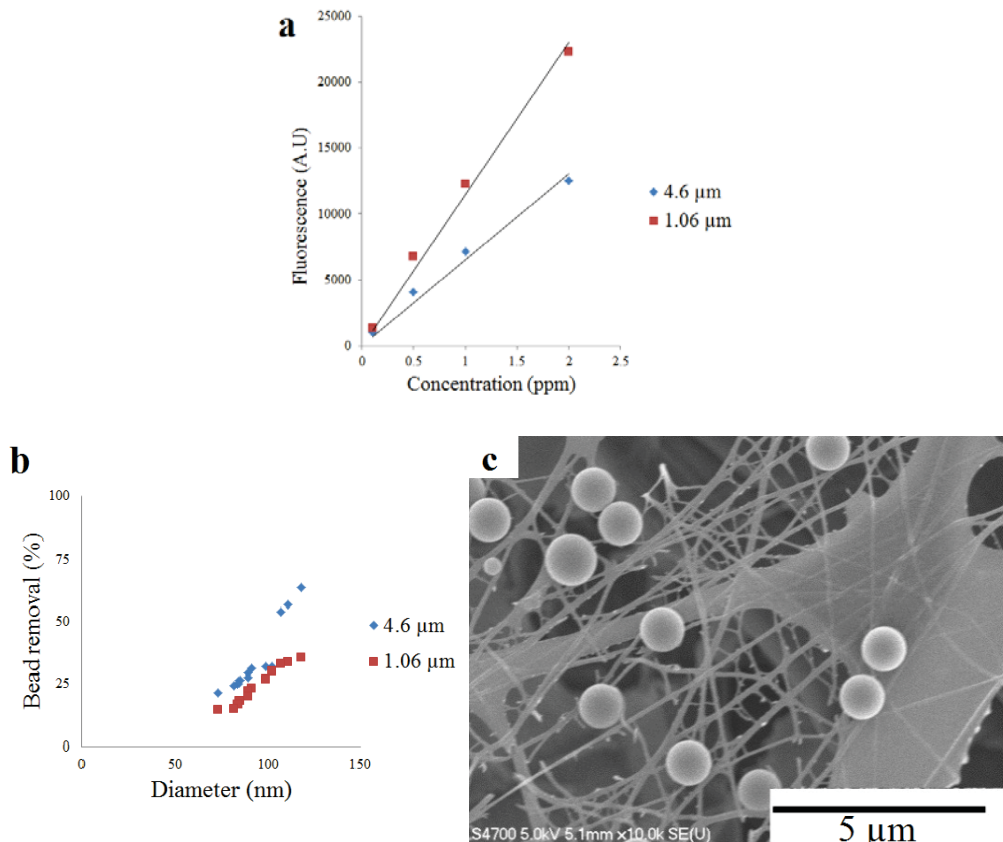
Figure 4.4Fluorescent beads filtered with various nanofibers. (a) Stand curve of fluorescent beads. (b) Bead removal as a function of nanofiber diameter. (c) SEM image of 1.1 μm diameter fluorescent beads filtered with nanofibers. The nanofibers were electrospun 2.5 wt% chitosan under 7.5 ml/h feed rate, 15 kV voltage, distance is 10 cm and the nanofibers are about 113 nm in diameter.

4.1.2 Virus adsorption of chitosan nanofibers

One of the most important goals in this thesis is to find a nanofiber that effectively removes virus. Here we used the virus porcine parvovirus (PPV). PPV has three kinds of proteins on the surface. There are 60 proteins on its surface, with 80% of them being the same protein, designated VP2 (viral protein 2) (Simpson et al. 2002). This provides multiple, identical binding sites on the virus surface and implies that adsorption is likely a good method to remove the virus. Parvovirus are difficult to inactivate under various heat and pH environments (Kempf et al. 2007), and are one of

the smallest known mammalian virus, with a diameter of 18-26 nm (Mengling 1999). These properties make them good models for virus removal techniques.

In order to evaluate the effectiveness of chitosan nanofibers on removing PPV, we used the MTT removal assay to measure virus concentration before and after contact with nanofibers. Polypropylene and filter paper were chosen as supports to collect the nanofibers. We measured virus removal to test the effect of these two media as a base of chitosan nanofibers on virus binding. According to Fig 4.5a, both polypropylene and filter paper bind virus less than 38% of virus. Since filter paper is much cheaper in water purification application, we used filter paper for all other work completed here. It was also disappointing that the electrospun chitosan/PEO in 90% acetic acid fibers did not appear to increase virus binding over the support paper.

Small volume tubes are used in the process of infecting virus, and we wanted to confirm that virus was binding to our samples and not to the tubes, so we compare the virus removal of various tubes without nanofibers present. The results can be found in Fig 4.5b. The tubes were Fisherbrand Premium Microcentrifuge Tubes, VWR® High-Performance Centrifuge Tubes, Nunc® CryoTube® Vials, and Corning Low Binding Microcentrifuge Tubes. Except for the low adhesion tubes, that only bound 6% of PPV, all other tubes can bind 58-77% PPV. In order to minimize the margin of error caused by tubes, low adhesion tubes were used in the process to test the virus removal of nanofibers.
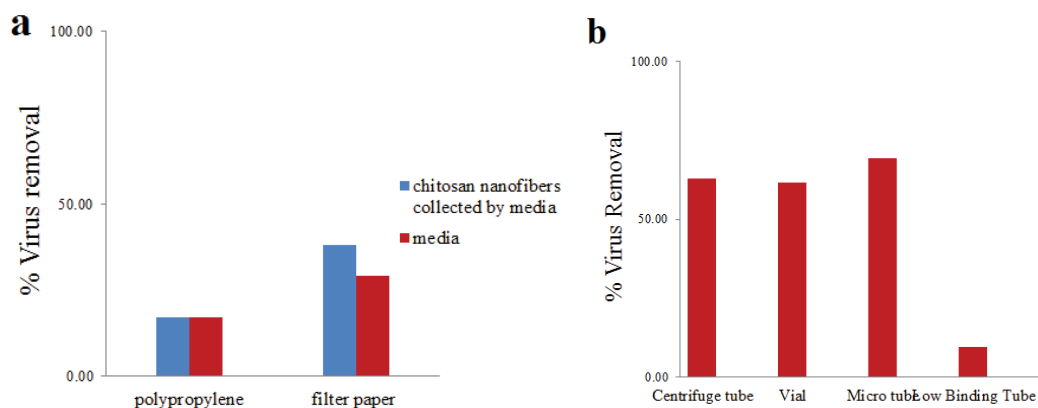
Figure 4.5 Removal of PPV. (a) Removal of PPV by chitosan nanofibers collected with different supports as compared to the plain supports. Concentration for all polymer blends was 9:1 chitosan/PEO blend solution at 2.5 wt% in 90% acetic acid. Electrospinning conditions were voltage of 20 kV, feed rate of 7.5 ml/h, and distance of 10 cm. (b) Removal of PPV by various tubes to conduct virus binding assays.

After showing low virus removal for chitosan (Fig 4.5a), we were interested in the influence of pH and fiber diameter on the removal of virus. PPV has a pKa of 5.3 (Weichert et al. 1998), and chitosan has a pKa of 6.5 (Lim and Hudson 2007). The hypothesis of binding PPV to chitosan nanofibers is electrostatic force, so between a pH of 5.3-6.5, the chitosan is positively charged and PPV is negatively charged. This pH range should produce the highest virus removal. First, we tried different pH buffer solutions for virus binding, as shown in Fig 4.6a. The results showed that pH 6-8 works better than pH 4-5. We are not sure why pH 7 and 8 showed the highest virus removal. Since the difference of virus removal value between each column is not big, the difference between the lower pH's (4-5) and the higher pH's (6-8) may not be significant. It is likely an error in the virus reduction assay and not a significant error.

In order to improve the virus binding to chitosan, which was shown to be very low in Fig 4.5a, we examined the effect of the electrospinning parameters shown in Fig 4.3 to change the fiber diameter on virus binding. We made two combination of chitosan blend solution, chitosan/PEO at a 9:1 ratio and a 8:2 ratio in 90% acetic acid.

38
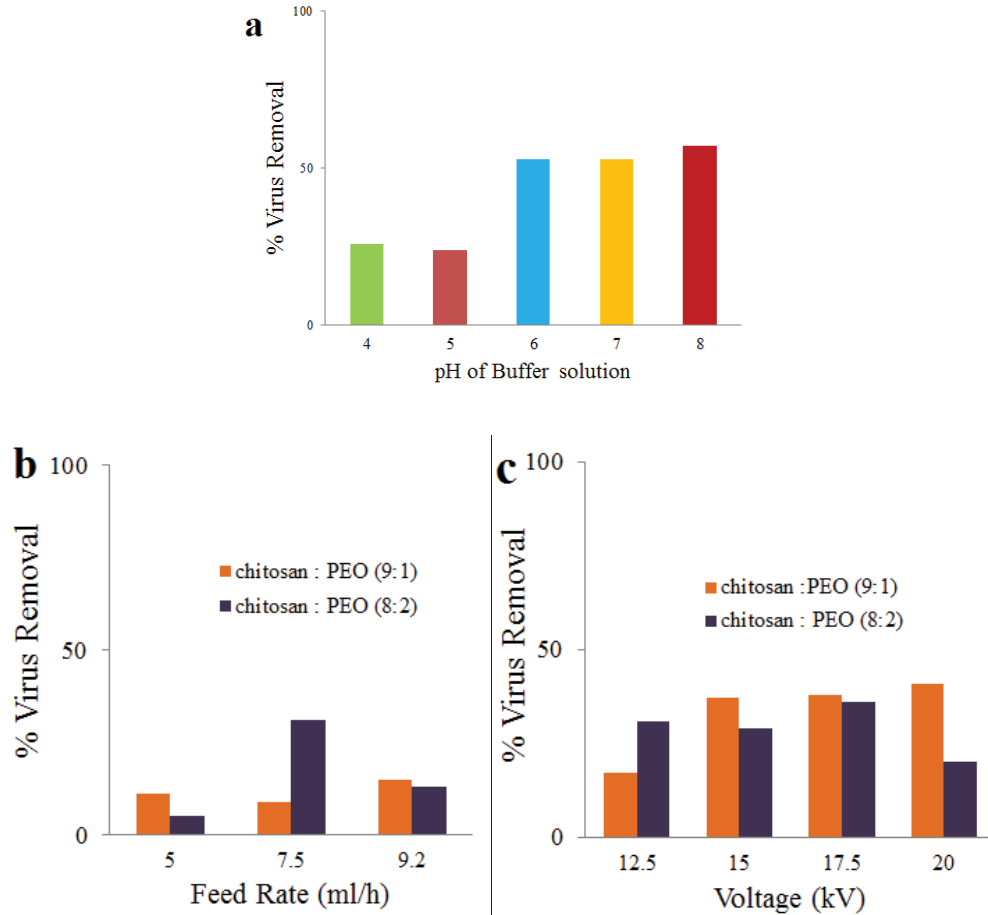
 Figure 4.5 Removal of PPV by chitosan nanofibers. (a) Effect of pH on virus removal. Nanofibers were produced by 9:1 chitosan/PEO blend solution in 90% acetic acid. Electrospinning conditions were voltage of 20 kV, feed rate of 7.5 ml/h, and distance of 10 cm. (b) Virus removals of nanofibers produced under various feed rates. Electrospinning conditions were voltages of 20 kV and distance of 10 cm. (c) Virus removals of nanofibers produced under various voltages. Electrospinning conditions are feed rate of 7.5 ml/h. Concentration for all chitosan/PEO blend solution in 90% acetic acid is 2.5 wt%.

According to Fig 4.6, after changing the variables of voltage, feed rate and concentration, unfortunately, chitosan nanofibers produced at 20 kV voltage and 7.5 ml/h feed rate could only remove a maximum of 40% PPV. No chitosan/PEO nanofibers were able to bind virus effectively since no condition showed over 90% (1 LRV) removal. The principle of binding virus to chitosan is that the nanofibers are positively charged and can bind the negatively charged virus. This hypothesiz was confirmed by the pervious experiments where 0.7 wt% chitosan in acetic acid solution had been incubated with four kinds of virus for 3 hours. The chitosan solution reduced phiX174 (Coliphage) by 1.19–

1.29 LRV, MS2 (coliphage) by 1.88–5.37 LRV, FCV-F9 (feline calicivirus) by 2.27–2.94 LRV, and MNV-1(feline calicivirus) by 0.09–0.28 LRV (Davis et al. 2012). It seems that chitosan works effectively for some virus, but not all kinds of virus. Unfortunately, after many attempts, we could not find effective chitosan nanofibers to bind more than 90% virus. We then began to explore increasing the positive charge to increase virus binding.

4.2   HTCC nanofibers

According to poor virus binding results found from electrospun chitosan, it was necessary to increase the positive charge of the polymer. The quaternized chitosan derivatives have N^+ groups so they contain a higher cationic nature, compared to the NH_2 groups of chitosan. We therefore chose to modify chitosan into quaternized chitosan. A quaternary ammonium derivative can be created and it is known for its antibacterial activity against a variety of bacteria and fungi (Alipour et al. 2009). HTCC (N-[(2-hydroxy-3-trimethylammonium) propyl] chitosan chloride) is one of the quaternized chitosan derivatives and we hypothesized that HTCC nanofibers could bind more virus, as compared to chitosan nanofibers. We started with the synthesis of HTCC and then tested HTCC nanofibers for their virus binding ability.

4.2.1 HTCC Synthesis and Characterization

HTCC was synthesized as described in section 3. Materials and Methods. After the synthesis was complete, it was necessary to determine the degree of quaternization. Three batches of HTCC solutions were titrated and the titration was performed three times for each batch with a value DQ of 78.1 ± 1.10%. FTIR (Fourier transform infrared spectroscopy) and NMR (nuclear magnetic resonance) were used to determine the chemical composition of the HTCC. The FTIR and NMR spectra of chitosan and HTCC are shown in Figs 4.7 and 4.8, respectively.
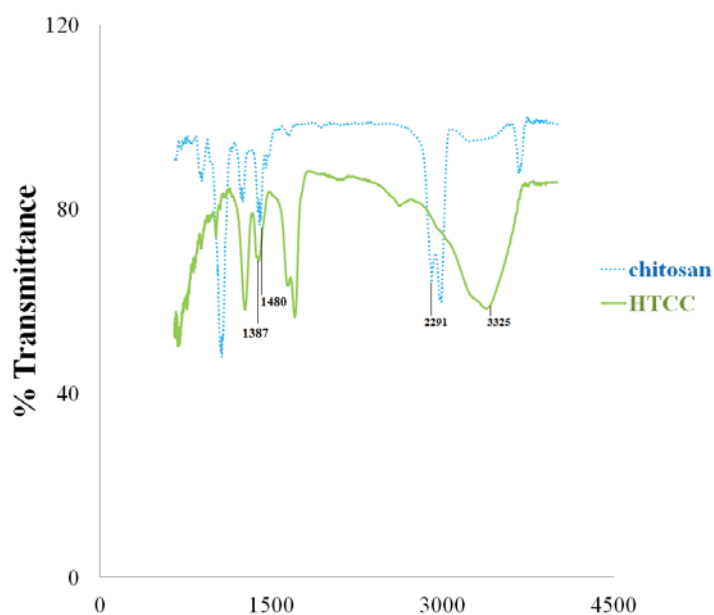
Figure 4.6 FTIR spectra of HTCC at 10 mg/ml in water and chitosan at 2 mg/ml in 90% acetic acid.

There are several peaks that proved existence of HTCC. A peak at 1387 cm^{-1} was assigned to the bending of CH_3. The peak at 1480 cm^{-1} was due to CH bending of trimenthyl ammonium group. The peak at 3325 cm^{-1} confirms the N-H stretching of a secondary amine. This peak can prove the synthesis of HTCC by forming N-H group. For chitosan, the peak at 2991 cm^{-1} represents the CH stretch (Alipour et al. 2009).

The concentration of chitosan solution for NMR is higher than FTIR. Low concentrations (2 wt%) could not obtain any peaks except for the solvent. For chitosan, the peak at 2.5 represent NH_2 group, the peaks between 3.4 and 4.2 confirm the hydrogen at secondary carbon atoms of the ring structure. For the HTCC spectra, the peak at 1.9 represents the NH group. Signal at 3.5 represents $^{+}N\text{-}CH_3$, and this is the formation of trimethyl group, the peak between 4.5 and 5.0 represent D_2O (Britto and Filho 2005).
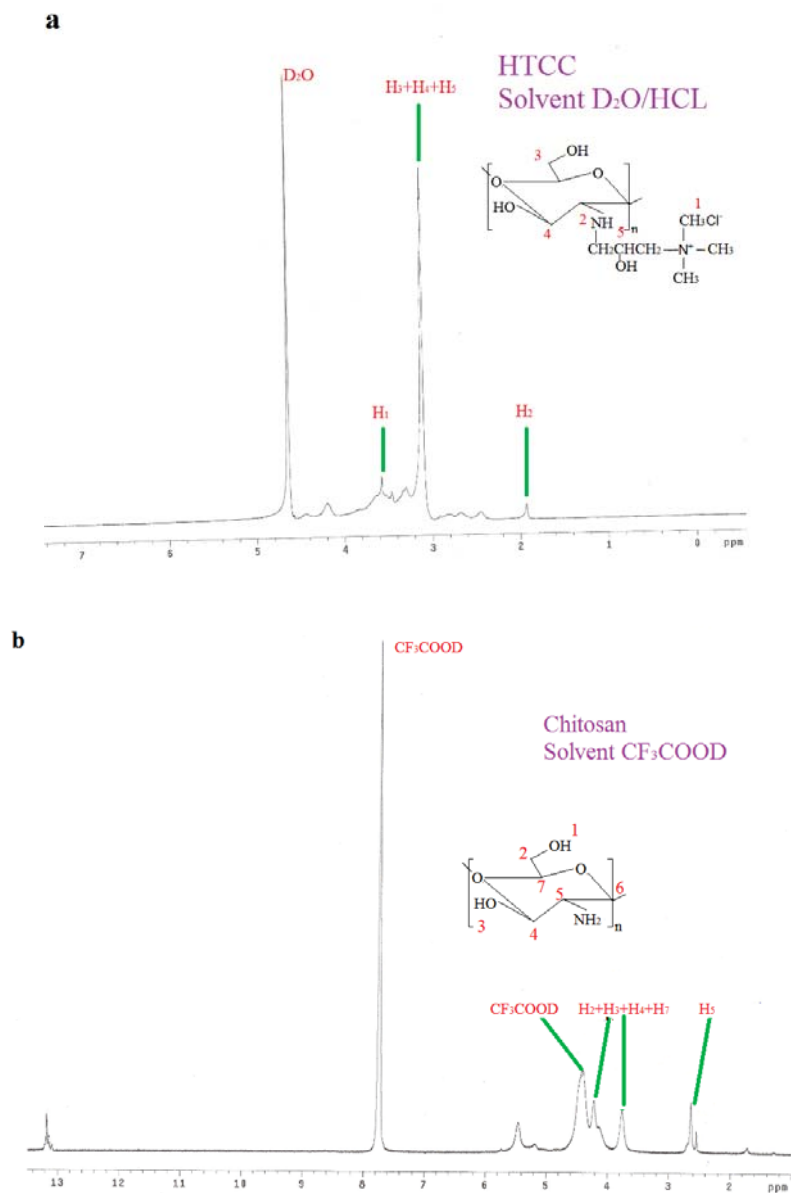
Figure 4.71H NMR spectra of HTCC (c = 10 mg/ml) dissolved in D2O/HCl (100/1 v/v) (a), and chitosan (c =5 mg/ml) dissolved in CF3COOD (b). (Courtesy of Xu Xiang)

4.2.2 Viscosity and conductivity of chitosan and HTCC solution

Chitosan derivatives are hard to electrospin because they have poor flexibility of their polyelectrolyte chains. To improve the electrospinning of the HTCC, we explored additives, similar to the work that was presented earlier on chitosan. These additives

42

change the conductivity, viscosity, surface tension, and crystallinity of the HTCC and can help to electorspin chitosan derivatives. We electrospun HTCC with four additives, included PEO, PVA, graphene and SDS. All of the additives were purchased and used as received, except for the graphene. The graphene was made by Xu Xiang, with similar protocol that has been published earlier (Murugan et al. 2009). The XRD image can be found in Fig 4.9. According to Fig 4.9, the peak at 24 Deg represents the existence of graphene. Graphene had one unique structure, a single layer of carbon atoms closely compacted into a two-dimensional (2D) honeycomb sp^2 carbon lattice. This peak explains the structure of graphene (Murugan et al. 2009).
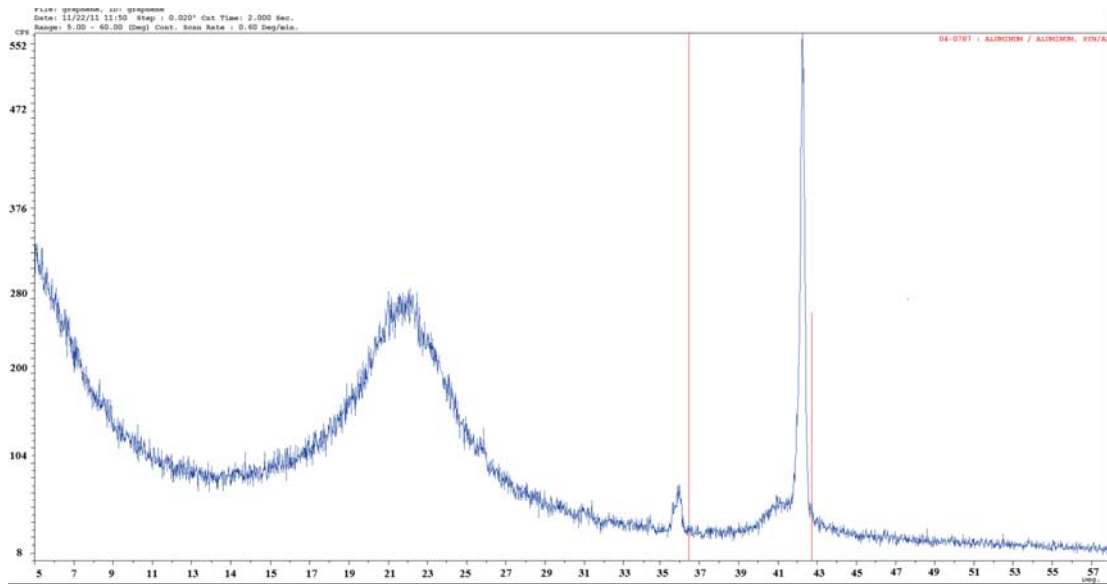

Figure 4.8 XRD (X-ray diffraction image) of graphene. (Courtesy of Xu Xiang)

In the electrospinning process, the electric force in the electrospinning system will pull the polymer solution out of the needle. The magnitude of the force can determine the degree of stretch of the jet. Both conductivity and viscosity can affect the electrospinning and the forming of a stable Taylor cone, which is required to form continuous and defect-free nanofibers. According to experiment observations, chitosan can be electrospun successfully, however, HTCC solutions could not be electrospun into fibers, additives are needed to improve HTCC electrospinning. There are several choices. First, graphene can increase the conductivity of HTCC. The structure of graphene is a 2D honeycomb sp^2 carbon atom and graphene has superb electronic conductivity, the charge

capacity of graphene can achieve 540 mAh g^{-1}. Graphene can also have a high surface area 2600 m^2 g^{-1} (Zhu et al. 2010), and this may attract hydrophobic patches on the virus surface. The second choice is SDS. It is negatively charged and can bind to chitosan to decrease the crystallinity (Zeng et al. 2003). This should also decrease the crystallinity of HTCC. Third, PVA is highly hydrophilic, has an inherent fiber- and film-forming ability, and can be easily cross-linked (Zhang et al. 2005). The last is PEO; it can be easily electrospun and decrease chitosan, and therefore HTCC, crystallinity (Homayoni et al. 2009). In order to determine which additive affected the electrospinning of HTCC, conductivity and viscosity were studied, as shown in Fig 4.10.
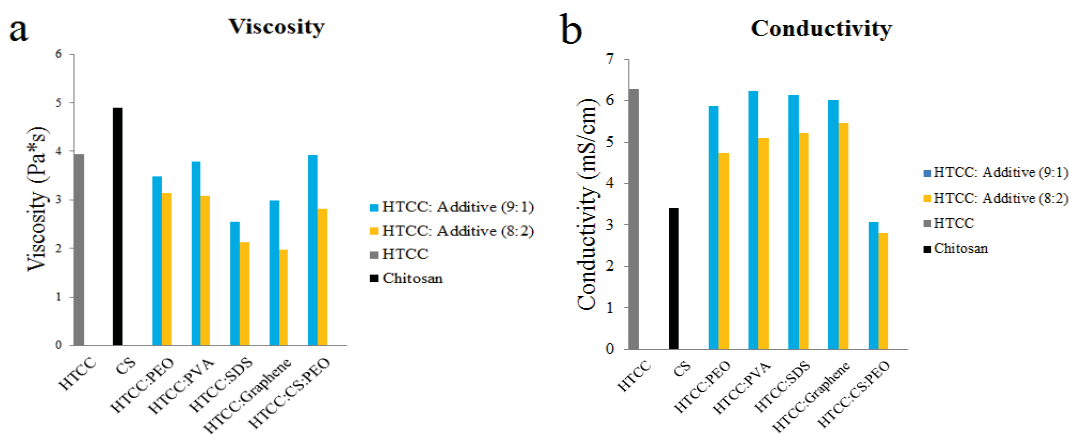

Figure 4.9 Viscosity and conductivity. The concentration for chitosan solution was 2.55 wt% in 90% acetic acid. The concentration for all HTCC/Additive blend solution was 10 wt% in water.

Please note that the concentration of the HTCC solutions are almost 5 times higher than the chitosan solutions. Pure chitosan has the highest viscosity among these combinations. As mentioned earlier, this is due to the increased crystallinity of chitosan caused by hydrogen bonding. As shown with chitosan, the blend viscosity and conductivity also increased with an increase of HTCC content. The results show that the viscosity of the HTCC blend solutions are lower than that of the chitosan solution, even though the concentration is almost 5-fold higher. This demonstrates that the difficulty of HTCC blend solutions to form a consistent nanofiber is likely due to the low viscosity. HTCC solutions had higher conductivity due to the increased positive charge on the HTCC, comparing to chitosan. Since both HTCC and chitosan solution can be

electrospun, we guess that conductivity higher than 3.2 mS/cm can be electrospun successfully. We hypothesize that HTCC nanofibers can bind more virus due to this increased positive charge.
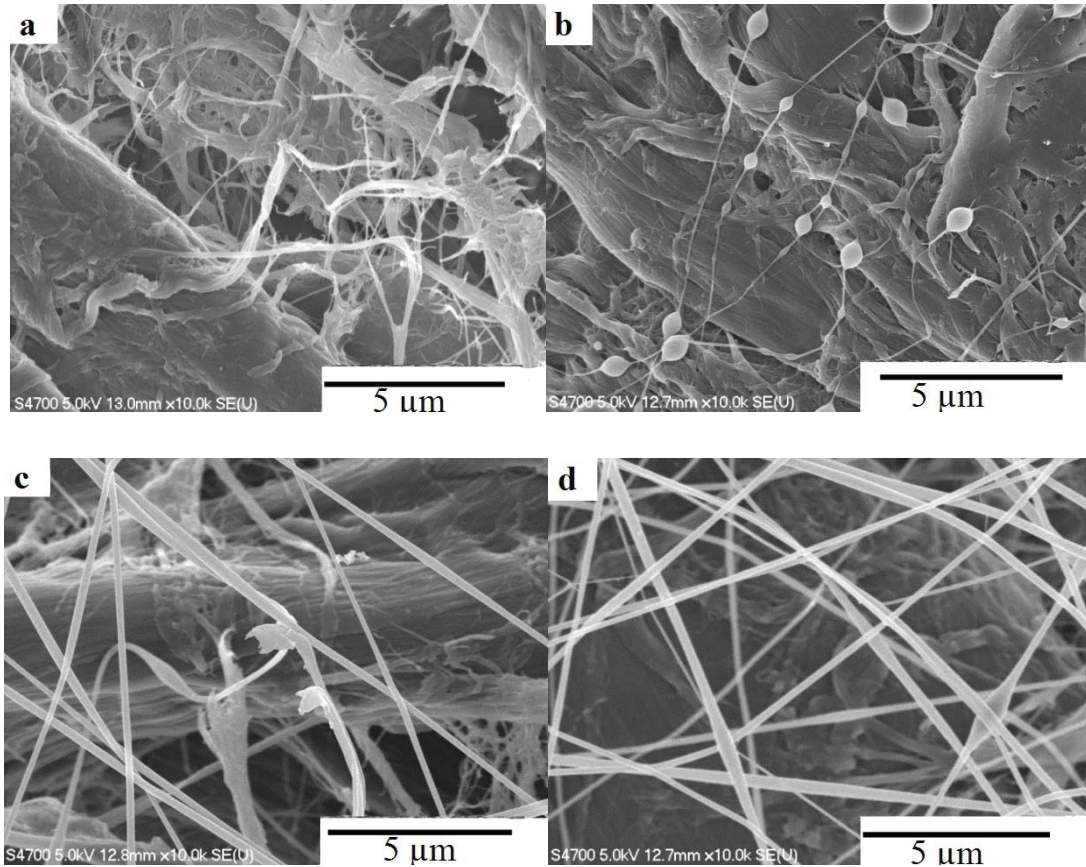

Figure 4.10 SEM micrographs of electrospun HTCC/graphene at various concentrations. The mass ratio is 9:1, feed rate is 6 ml/h, distance is 10 cm and voltage is 20 kV. The concentration for each sample is (a) 5 wt%, (b) 7 wt%, (c) 10 wt%, and (d) 12 wt% in water.

From Fig 4.11, we can see that low concentrations of HTCC blends yielded either a few fibers that contain beads (7 wt%) or no fibers at all (5 wt%), likely due to the low viscosity. It is concluded that clear and defect-free fibers can be seen at a concentration of 10 wt% or higher. The average diameter increased from 113 ± 41 nm at 7 wt% to 330 nm ± 54 nm at 10 wt% to 390 ± 27 nm at 12 wt%. The fiber diameter increased with increasing concentration of blend solution, likely due to the increase in viscosity. This

shows that electrospun solutions must maintain a high viscosity to form continuous, defect-free fibers. For electrospun fiber of HTCC with the other additives, no nanofibers were observed. For this reason, we pursued graphene as our additive of choice.

4.2.3 Virus adsorption of HTCC

A series of HTCC electrospun support filters with the different additives have been studied for their ability to remove PPV. Pure HTCC solutions in water are hard to electrospun, it's hard to form Taylor Cone in electrsopinning process. Based on this, we need to choose additives to help electrospinning. It is likely that pure HTCC in water does not form nanofibers, but enough HTCC is attached to the support filter to increase virus removal. The results of virus removal by HTCC blended with various additives can be found at Fig 4.12. Table 4.1 and Table 4.2 show the LRV of each condition in Fig 4.12. Concentration of chitosan/PEO is 2.5 wt% in 90% acetic acid and the mass ratio is 9:1.
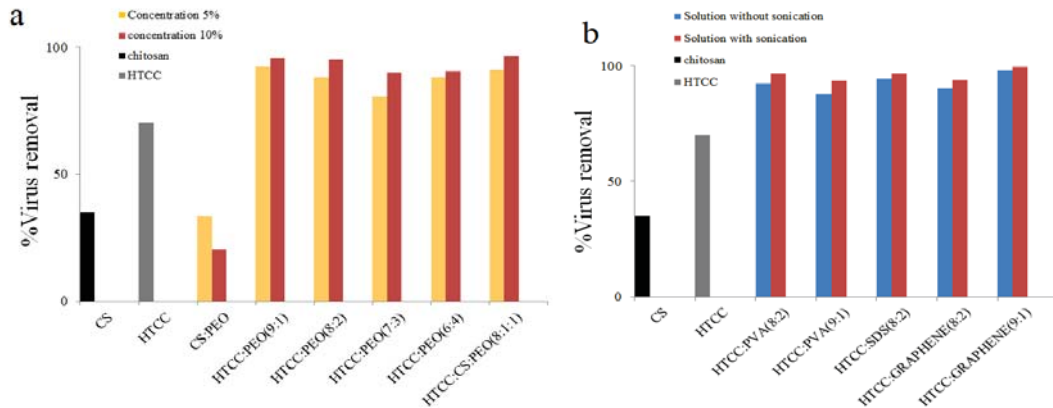
Figure 4.12 Virus removal of PPV by HTCC blends. (a) Virus removal of HTCC nanofibers with various additives at concentrations of 5 wt% and 10 wt% in water, concentration of chitosan and chitosan/PEO concentrations are 2.5 wt% in 90% acetic acid (b) Virus removal of HTCC and chitosan nanofibers with various additives with and without sonication, concentration of HTCC is 10 wt% in water, concentration of chitosan and chitosan/PEO in 90% acetic acid concentrations are 2.5 wt%, feed rate is 6 ml/h, distance is 10cm and voltage is 20 kV

According to Fig 4.12a, pure HTCC nanofibers can remove much more PPV than pure chitosan, but the virus removal is still lower than 90% (1 LRV). After adding 10

wt% graphene of the total solid, HTCC blend nanofibers can remove up to 99% virus. Among various additives, graphene works best on virus removal, HTCC/graphene blend solutions in water are easy to electrospinning, compared to other combinations. Sonication of the blends also assisted in the formation of uniform solutions. This was shown by the improvement of virus removal with polymer blends that were sonicated, as compared to nonsonicated samples Fig 4.12b. Error bars on are not present because this experiment was only done once.

Table 4.1
Virus removal of HTCC nanofibers blended with additives at various concentration

Polymer	CS:PEO	HTCC:PEO (9:1)	HTCC:PEO (8:2)	HTCC:PEO (7:3)	HTCC:PEO (6:4)	HTCC:CS:PEO (8:1:1)
concentration						
5%	33.6	92.3	88.2	80.6	88.2	91
10%	20.5	95.7	95.3	90.1	90.5	96.5

Table 4.2
Virus removal of HTCC nanofibers blended with additives after sonication

Sonication	HTCC:PVA (8:2)	HTCC:PVA (9:1)	HTCC:SDS (8:2)	HTCC:GRAPHENE (8:2)	HTCC:GRAPHENE (9:1)
No	92.5	87.8	94.4	90.3	98.1
Yes	96.6	93.4	96.6	93.6	99.5

In the virus removal assay, the pH of the buffer solution for chitosan and HTCC was the same at a pH of 7, in order to keep all parameter are same. The pKa of quaternized amine is around 10 (Leach et al. 2012) and the pKa of chitosan is 6.5 (Lim and Hudson 2007). At pH 7, which is the pH of the buffer solution, HTCC is fully positively charged and chitosan is close to neutral. Since HTCC is positively charged, it can explain the higher virus removal of HTCC nanofiber than chitosan nanofiber.

Due to the high virus removal capability of the HTCC/graphene blend and the ability to form nanofibers (Fig 4.11), we chose graphene as the additive to continue to study. Among various additives, graphene with HTCC can be electrospun, because graphene does not block the needle during electrospinning. Other additives blocked the

needle and impeded the electrospinning. In the electrospinning process, droplets fell from the needle instead of being propelled towards the grounded collector, which reduced the formation of nanofibers. HTCC/graphene nanofibers were not as easy to electrospin as compared to chitosan solutions. In order to get more naofibers, we electrospun with longer time and adjusted the concentration of HTCC solution. The SEM images of electrospun HTCC/graphene (9:1) in water can be found in Fig 4.13.
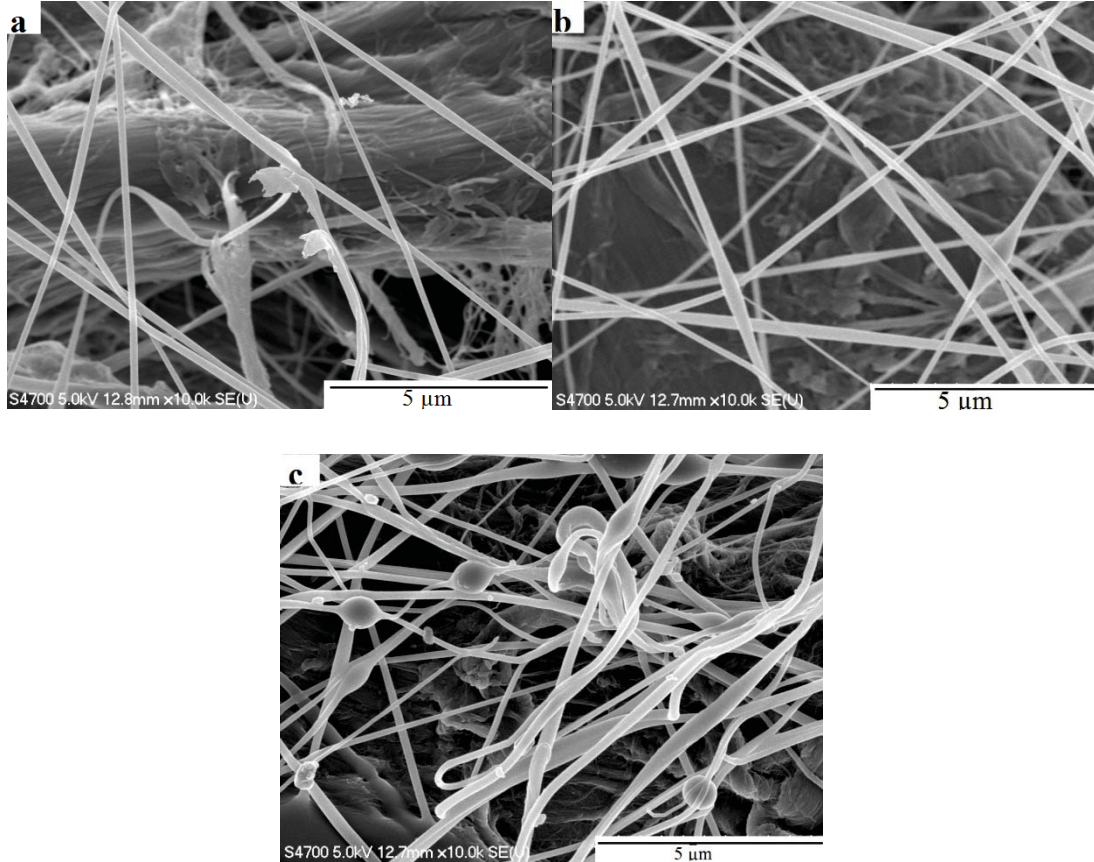

Figure 4.11SEM micrographs of electrospun HTCC/graphene in water at various electrospun times.The mass ratio is 9:1, feed rate is 6 ml/h, distance is 10 cm and voltage is 20 kV. The concentration for each sample is 12 wt% in water. The electrospinning time is (a) 18 mins, (b) 36mins, (c) 54mins.

The SEM image can be found in Fig 4.13 and the virus removal results can be found in Fig 4.14. According to Fig 4.13, we can measure the fiber density of HTCC nanofibers electrospun under different time. The method of measuring fiber density can be found in the section 3. Material and Method. The fiber density in the units of

fibers/μm^2 was found to be 0.249 ± 0.023, 0.012 ± 0.012, 0.083 ± 0 corresponding to nanofibers electrospun for 54 mins, 36 mins and 18 mins, respectively, based on the calculation from two SEM images. It was concluded that increasing electrospinning time can increase fiber density. This demonstrates that we can control the fiber density and make various grades of nanofiber filter by controlling the electrospinning time. This conclusion had been comfirmed by the electrospingn of polyacrylonitrile (PAN) fibers (MyoungYun et al. 2007). The virus removal assay with electrospun HTCC/graphene (9:1) in water under various time and concentration can be found in Fig 4.14.
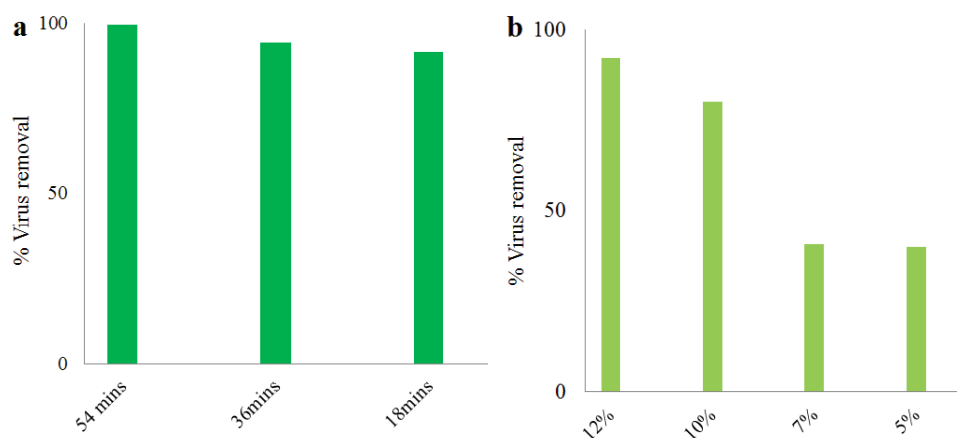

Figure 4.12 Virus removal of HTCC blends in water at different times and concentrations.(a) Virus removal of electrospun HTCC/graphene (12 wt%) in water at mass ratio of 9:1 under different electrospinning time.   (b) Virus removal of HTCC/graphene blend nanofibers at mass ratio of 9:1 under various concentrations. Feed rate is 6 ml/h, distance is 10cm and voltage is 20 kV

Longer electrospinning time increases the binding ability of HTCC/graphene nanofibers due to an increase in nanofibers per unit area. More nanofibers have a higher number of amine groups and increased charge, and therefore more virus adsorption capacity. This result is confirmed by Fig 4.14. Electrospun HTCC blends at 12 wt% can bind more PPV, comparing to electrospun 5 wt% HTCC blend. Higher conductivity of solution will cause a higher charge of the surface of the ejected jet via electrospinning. Postively charged nanofibers absorb more PPV.

We used the Langmuir isotherm model to study the equilibrium adsorption of virus to nanofibers. For PPV, one virus partical is equal to 1 MTT unit (Heldt et al.

49

2006). Based on equation 3.3, on a plot of C/q versus c, the slope is $1/q_{max}$ and the intercept is K_d/q_{max}. The plot of the linearized Langmuir isotherm is shown in Fig 4.15 and we found the K_d value to be 6.6×10^{-21}M. The strongest binding ability of protein has a measured K_d value of 10^{-14} M for the binding of strepavidin and biotin (Green. 1975). HTCC had been proved ability to adsorb PPV in Fig 4.14, but the calculated K_d value does not reflect a realistic value. This may be due to the method used to determine the fiber density and fiber surface area was not accurate, since this was calcualted from only two SEM images. Another possibility is that the Langmuir model is not a valid model for our system. There could be non-homogenous binding sites or multiple layer binding.
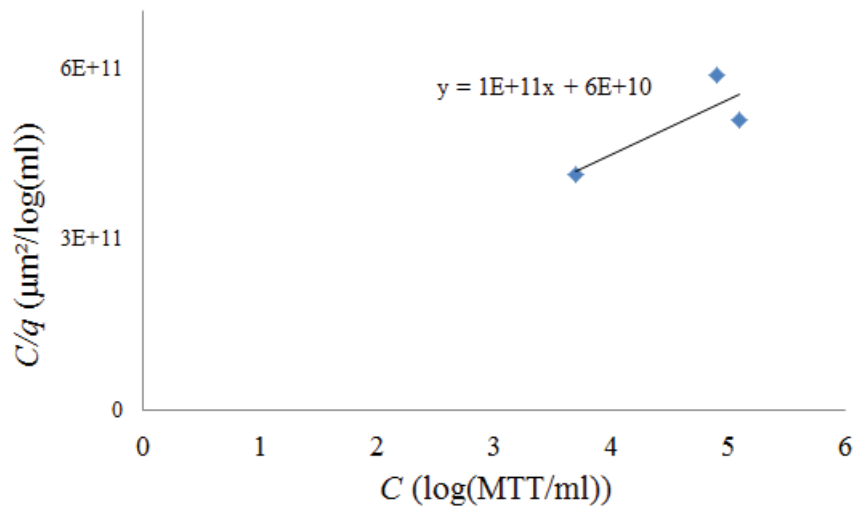
Figure 4.13 Langmuir model of HTCC nanofibers

Chitosan solutions can be electrospun successfully, but could not bind virus effectively, therefore, we modified the chitosan into HTCC and electrospun HTCC solutions in water. For HTCC nanofibers, 10-12 wt% of a 9:1 HTCC/graphene blend solution in water can be electrospun successfully and effectively remove 99% of virus. SEM images showed that HTCC/graphene nanofibers had defect-free fibers with 330-390 nm diameters.

5 Conclusion & Future work

Among various combinations of chitosan and HTCC nanofibers, HTCC/graphene in water can be electrospun successfully and remove 99% of PPV. Chitosan nanofibers can only remove up to 50% virus. Although chitosan nanofibers can be electrospun easily and successfully, HTCC nanofibers are preferred for water purification technology.

In order to apply electrospun membranes in filtration, chemistry and morphology of the fibers are important. The relation between voltage, feed rate, and concentration to diameter has been examined here. Smaller diameter fibers produce a higher surface area, therefore increasing the binding surface for PPV. For electrospun chitosan/PEO in 90% acetic acid fibers, the diameter increases with increasing feed rate and diameter decreases with increasing voltage. The average diameter of electrospun chitosan fibers is in the range of 80-130 nm. For HTCC/graphene fibers, the diameter increases with increasing concentration. The average diameter of electrospun HTCC blend fibers is in the range of 330-390 nm. Right now, we can only obtain nanofiber electrospun from HTCC/graphene. Increase electrospinning time can increase the fiber density and increased fiber density increases virus removal. HTCC/graphene fibers can remove 99% of PPV in solution, and therefore have the potential to become a future water purification technology.

The main future work will focus on increasing the effectiveness of electrospinning HTCC nanofibers and increasing the virus removal capability of HTCC nanofibers. In the electrospinning process, chitosan blend solutions are more effective than HTCC blend solution. This can be explained by the lower conductivity and higher viscosity. HTCC has a lower viscosity than chitosan. Electrostatic force cannot exceed the surface tension of HTCC solution or pump flow rate is low and droplets in the tip of the needle do not reach the grounded collector. Inconsistent flows reduce the nanofibers that can be collected. In order to increase the electrospinning effectiveness of HTCC

blend solutions, appropriate voltage is needed. Increasing the concentration of HTCC is also an option.

Another method to improve the virus binding of electrospun fibers is to add affinity ligands to the fibers. Small binding peptide ligands have shown the ability to remove PPV in previous studies (Heldt et al. 2008). We hypothesized that adding peptides (WRW and KYY) to chitosan amine groups may increase the binding ability of chitosan nanofibers, as compared to HTCC nanofibers. WRW and KYY peptides each have two hydrophobic and one positively charged amino acid group. Peptides are preferred to proteins, like antibodies, as affinity ligands because they are stable and lack second structure (Heldt et al. 2009).

The third one will focus on the analysis of virus removal with nanofibers. The Langmuir isotherm will be applied to virus adsorption of fibers of different densities and different fiber diameters. This will give us a more complete picture of virus adsorption to nanofibers.

6 References

Alipoura SM, Nouria M, Mokhtaria J, Bahramib SH. 2009. Electrospinning of poly (vinyl alcohol)–water-soluble quaternized chitosan derivative blend. Carbohydrate Research. 344(18): 2496-2501

Areias AC, Ribeiro C, Sencadas V, Giralt N, Perez A, Ribelles JL, Méndez S. 2012. Influence of crystallinity and fiber orientation on hydrophobicity and biological response of poly (L-lactide) electrospun mats. Soft Matter. 8(21): 5118-5825.

Barnes CP, Sell SA, Boland ED, Simpson DG, Bowlin GL. 2007. Designing the next generation of tissue engineering scaffolds. Nanofiber technology. 59(14): 1413–1433.

Bennett A. 2008. Pathogen removal from water–technologies and techniques. Filtration and Separation. 45(10): 14-16.

Bhattarai N, Edmondsona D, Veiseha O, Matsenb FA, Zhang M. 2005. Electrospun chitosan-based nanofibers and their cellular compatibility. Biomaterials. 26: 6176–6184.

Brehant A, Glucina K, Moigne I. Mental validation using Ms2-phages.Desalination. 250(3): 956–960.

Britto D, Filho SP. 2005. Mechanical Properties of N, N, N-trimethylchitosan Chloride Films. Polímeros: Ciência e Tecnologia. 15(2): 142-145.

Buchko CJ, Chen LC, Yu S, Martin DC. 1999. Processing and microstructural characterization of porous biocompatible protein polymer thin films. Polymer. 40: 7397-7407.

Chang R. 2010. Chemistry, 10th ed. McGraw-Hill Companies. 1168p.

Chatelet C, Damour O, Domard A. 2001. Influence of the degree of acetylation on some biological properties of chitosan films. Biomaterials. 22(3): 261–268

Chen Z, Mo X, Qing F. 2007. Electrospinning of collagen–chitosan complex. Materials Letters. 61(16): 3490-3494.

Chuangchote S, Supaphol P. 2006. Fabrication of aligned poly (vinyl alcohol) nanofibers by electrospinning. Nanoscience and Nanotechnol. 6(1): 125-129.

Crini G. 2005. Recent developments in polysaccharide-based materials used as adsorbents in wastewater treatment. Progress in Polymer Science. 30(1): 38–70.

Crisafully R, Milhomed MAL, Cavalcante RM, Silveir ER, Keukeleire DD, Nascimento F. 2008. Removal of some polycyclic aromatic hydrocarbons from petrochemical wastewater using low-cost adsorbents of natural origin. Bioresource Technology. 99(10): 4515–4519.

Davis R, Zivanovic S, Dsouza D, Davidson P. 2012. Effectiveness of chitosan on the inactivation of enteric viral surrogates. Food Microbiology. 32(1): 57-62.

Deitzel JM, Kleinmeyer J, Harris D, Tan NCB. 2001. The effect of processing variables on the morphology of electrospun nanofibers and textiles. Polymer. 42: 261-264.

Delgrange VN, Cabassud C, Cabassud M, Bourlier LD, Laínê JM. 2000. Neural networks for long term prediction of fouling and backwash efficiency in ultrafiltration for drinking water production. Desalination. 131(1): 179-188.

Dotti F, Varesano A, Montarsolo A, Aluigi A, Tonin C, Mazzuchetti G. 2007. Electrospun Porous Mats for High Efficiency Filtration. Journal of Industrial Textiles. 37(2): 151-162.

Duan B, Yuan X, Zhu Y, Zhang Y, Li X, Zhang Y, Yao K. 2006. A nanofibrous composite membrane of PLGA–chitosan/PVA prepared by electrospinning. European Polymer Journal. 42: 2013–2022.

Environmental Protection Agency (EPA). 2007. The Long Term 2 Enhanced Surface Water Treatment Rule (LT2ESWTR) Implementation Guidance. LT2ESWTR Toolbox Guidance Manual. 7-8.

Fang J, Wang X, Lin T. 2011. Functional Applications of Electrospun Nanofibers. Nanofibers - Production, Properties and Functional Applications. 14: 287-302.

Fang SW, Li CF, Shih DYC. 1994. Antifungal activity of chitosan and its preservative effect on low-sugar candied kumquat. Food Protect. 56 (2): 136–140.

Fridrikh SV, Yu JH, Brenner MP, Rutledge GC. 2003. Controlling the Fiber Diameter during Electrospinning. Physical Review Letters. 90: 144-150.

Geng XY, Kwon OH, Jang JH. 2005. Electrospinning of chitosan dissolved in concentrated acetic acid solution. Biomaterials. 26: 5427-5230.

Green N. M. 1975. Review article. Advances in Protein Chemistry. 29: 85-133.

Guibal E, Roussy J. 2007. Coagulation and flocculation of dye-containing solutions using a biopolymer (Chitosan). Reactive & Functional Polymers. 67: 33–42.

Guibal E, Vooren MV, Dempsey BA and Roussy J. 2006. A Review of the Use of Chitosan for the Removal of Particulate and Dissolved Contaminants. Separation Science and Technology. 41(11): 2487-2514.

Guibal E. 2004. Interactions of metal ions with chitosan-based sorbents: a review. Separation and Purification Technology. 38(1): 43–74.

Helander IM, Lassila EL, Ahvenainen R, Rhoades J, Roller S. 2002. Chitosan disrupts the barrier properties of the outer membrane of Gram-negative bacteria. International Journal. 71(2): 235–244.

Heldt CL, Gurgel PV, Jaykus LA, Carbonell RG. 2008. Identification of Trimeric Peptides That Bind Porcine Parvovirus from Mixtures Containing Human Blood Plasma. Biotechnology Progress. 24(3): 554–560.

Heldt CL, Hernandez R, Mudiganti U, Gurgel PV, Brown DT, Carbonell R.G. 2006. A colorimetric assay for viral agents that produce cytopathic effects. Journal of Virological Methods. 135 (1): 56–65.

Homayoni H, Ravandi SAH, Valizadeh M. 2009. Electrospinning of chitosan nanofibers: Processing optimization. Carbohydrate Polymers. 77: 656–661.

Huang ZM, Zhang YZ, Kotaki M, Ramakrishna S. 2003. A review on polymer nanofibers by electrospinning and their applications in nanocomposite. Composites Science and Technology. 63: 2223.

Hwang JK, Kim HJ, Yoon SJ, Pyun YR. 1999. Bactericidal activity of chitosan on E. coli. In Advances in Chitin Science. 62(3): 239-243.

Ignatious. 2002. Electrospun amorphous pharmaceutical compositions. U.S. Patent No.60/401,726, filed on Aug 7, 2002. Philadelphia, PA: U.S.

Inmaculada A, Mengíbar M, Harris R, Paños I, Miralles B, Acosta N, Galed G, Heras A. 2009. Functional Characterization of Chitin and Chitosan. Current Chemical Biology. 3: 203-230.

Jeon YJ, Park PJ, Kim SK. 2001. Antimicrobial effect of chitooligosaccharides produced by bioreactor. Carbohydrate Polymers. 44(1): 71–76.

Jia Z, Shen D, Xu W. 2001. Synthesis and antibacterial activities of quaternary ammonium salt of chitosan. Carbohydrate Research. 333(1): 1–6.

Jiang HL, Fang DF, Hsiao BS, Chu B, Chen WL. 2004. Optimization and characterization of dextran nanofibers prepared by electrospinning. Biomacromolecules. 5: 326-331.

Jin HJ, Fridrikh SV, Rutledge GC, Kaplan DL. 2002. Electrospinning Bombyx mori Silk with Poly (ethylene oxide). Biomacromolecules. 3: 1233-1239.

Kempf C, Stucki M, Boschetti N. 2007. Pathogen inactivation and removal procedures used in the production of intravenous immunoglobulins. Biologicals. 35: 35-42.

Kendra DF, Hadwiger LA. 1984. Characterization of the smallest chitosan oligomer that is maximally antifungal to Fusarium solani and elicits pisatin formation in Pisum sativum. Experimental Mycology. 8(3): 276-281.

Kenawy ER, Bowlin GL, Mansfield K, Layman J, Simpson DG, Sanders EH. 2002. Release of tetracycline hydrochloride from electrospun poly (ethylene-co-vinylacetate), poly (lactic acid), and a blend. Journal of Controlled Release. 81: 57–64.

Kenawy ER, Layman JM, Watkins JR, Bowlin GL, Matthews JA, Simpson DG. 2003. Electrospinning of poly (ethylene-covinyl alcohol) fibers. Biomaterials. 24: 907–913.

Ki CS, Baek DH, Gang KD, Lee KH. 2005. Characterization of gelatin nanofiber prepared from gelatin–formic acid solution. Polymer. 46(14): 5094–5102.

Kim HS, Kim K, Jin HJ, and Chin IJ. 2005. Morphological characterization of electrospun nano-fibrous nanofibers of biodegradable poly (L-lactide) and poly (lactideco- glycolide). Macromolecular Symposia. 224: 145-154.

Kim J, Bruggen B. 2010. The use of nanoparticles in polymeric and ceramic membrane structures: Review of manufacturing procedures and performance improvement for water treatment. Environmental Pollution. 58(7): 2335–2349.

Kofuji K, Qian CJ, Nishimura M, Sugiyama I, Murata Y, Kawashima S. 2005. Relationship between physicochemical characteristics and functional properties of chitosan. European Polymer Journal. 41(11): 2784–2791.

Kozlov M, Moya W, Tkacik G. 2012. Removal of microorganisms from samples using nanofibers filtration media. PCT No. :PCT/US10/00826. Pub. No. : US 2012/0091072 A1.

Kulish EI, Volodina VP, Kolesov SV, Zaikov GE. 2006. Enzymatic degradation of chitosan films by collagenase. Polymer Science. 48: 9-10.

Kurita K, Kojima T, Nishiyama Y, Shimojoh M. 2000. Synnthesis and Some Properties of Nonnatural Amino Polysaccharides: Branched Chitin and Chitosan. Macromolecules. 33 (13): 4711–4716.

Lapitsky Y, Zahir T, Shoichet M. 2008. Modular Biodegradable Biomaterials from Surfactant and Polyelectrolyte Mixtures. Biomacromolecules. 9: 166–174.

The chemogenesis web book. 2012. The Lewis Acid/Base Interaction Matrix. Salford, UK: Dr Mark R. Leach. The Chemogenesis WebBook; [updated 2012, cited 2012]. Available from: http://www.meta-synthesis.com/webbook.html

Li H, Wu C, Tepper F, Lee J, Lee C. 2009. Removal and retention of viral aerosols by a novel alumina nanofiber filter. Journal of Aerosol Science. 40(1): 65-71.

Li L, Hsieh YL. Chitosan bicomponent nanofibers and nanoporous fibers. 2006. Carbohydrate Research. 341(30): 374–381.

Li WJ, Laurencin CT, Caterson EJ, Tuan RS, Frank K. 2002. Electrospun nanofibrous structure: A novel scaffold for tissue engineering. Journal of Biomedical Materials Research. 60(4): 613–621.

Lim SH, Hudson SM. 2003. Review of chitosan and Its Derivatives as Antimicrobial Agents and Their Uses as Textile chemicals. Journal of Macromolecular Science. 43(2): 223–269.

Liu XF, Guan YL, Yang DZ, Li Z, Yao KD. 2001. Antibacterial action of chitosan and carboxymethylated chitosan. Journal of Applied Polymer Science. 79: 1324–1335.

Ma H, Burger C, Hsiao B, Chu B. 2011. Ultra-fine cellulose nanofibers: new nano-scale materials for water purification. Journal of Materials Chemistry. 21: 7507-7510.

Megelski S, Stephens JS, Chase DS, Rabolt JF. 2002. Micro and Nanostructured Surface Morphology on Electrospun Polymer Fibers. Macromolecules. 35 (22): 8456–8466.

McKee MG, Wilkes GL, Colby RH, Long TE. 2004. Correlations of Solution Rheology with Electrospun Fiber Formation of Linear and Branched Polyesters. Macromolecules. 37 (5): 1760–1767.

McManus MC, Boland ED, Simpson DG, Barnes CP, Bowlin GL. 2007. Electrospun fibrinogen: feasibility as a tissue engineering scaffold in a rat cell culture model. Journal of Biomedical Materials Research Part A. 81(2): 299-309.

Meinel AJ, Germershaus O, Luhmann T, Merkle HP, Meinel L. 2002. Electrospun matrices for localized drug delivery. Current technologies and selected biomedical applications. 81(1): 1–13.

Mengling WL, Ed. 1991. Porcine Parvovirus. Diseases of Swine; Ames. IA: Iowa State University Press.

Morrica A, Nardini C, Falbo A, Bailey AC, Bucci E. 2003. Manufacturing process of Anti-thrombin III concentrate: viral safety validation studies and effect of column re-use on viral clearance. Biologicals. 31(3): 165–173.

Murugan AV, Muraliganth T, Manthiram A. 2009. Rapid, Facile Microwave-Solvothermal Synthesis of Graphene Nanosheets and Their Polyaniline Nanocomposites for Energy Strorage. Chemistry of Materials. 21: 5004–5006.

Myoung YK, Hogan C, Matsubayashi Y, Kawabe M, Iskandara F, Okuyamaa K. 2007. Nanoparticle filtration by electrospun polymer fibers. Chemical Engineering Science. 62: 4751 – 4759.

Ngah W, Kamari A, Koay YJ. 2004. Equilibrium and kinetics studies of adsorption of copper (II) on chitosan and chitosan/PVA beads. International Journal of Biological Macromolecules. 34(3): 155–161.

Ohkawa K, Cha D, Kim H, Nishida A, Yamamoto H, Macromol. 2004. Electrospun chitosan-based nanofibers and their cellular compatibility. Macromolecular Rapid Communications. 25: 1600–1605.

Pandey SJ, Jegatheesan V, Baskaran K, Shu L. 2012. Fouling in reverse osmosis (RO) membrane in water recovery from secondary effluent: a review. Reviews in Environmental Science and Biotechnology. 11: 125–145.

Park WH, Jeong L, Yoo D, Hudson S. 2004. Effect of chitosan on morphology and conformation of electrospun silk fibroin nanofibers. Polymer. 45: 7151–7157.

Prabhakaran MP, Venugopal JR, Chyan TT, Hai LB, Chan CK, Lim AY, Ramakrishn S. 2008. Electrospun biocomposite nanofibrous scaffolds for neural tissue engineering. Tissue Engineering Part A. 14: 1787–1797.

Qin XH, Wang SY. 2008. Electrospun Nanofibers from Crosslinked Poly (vinyl alcohol) and Its Filtration Efficiency. Journal of Applied Polymer Science. 109: 951–956.

Qing H, Kai G, Qiang A, Tuo M, Yu F, Yan G, Xiu F. 2011. Positive charge of chitosan retards blood coagulation on chitosan films. Journal of Biomaterials Applications. 1–14:22-59.

Rinaudo, M. 2006. Chitin and chitosan: Properties and applications .Progress in Polymer Science. 31: 603–632.

Riordan W, Heilmann S, Brorson K, Seshadri K, He Y, Etzel M. 2009. Design of Salt-Tolerant Membrane Adsorbers for Viral Clearance. Biotechnology and Bioengineering. 103(5): 920-929.

Sato A, Wang R, Ma H, Hsiao B, Chu B. 2011. Novel nanofibrous scaffolds for water filtration with bacteria and virus removal capability. Journal of Electron Microscopy. 60(3): 201–209.

Šćiban M, Radetić B, Kevrešan Z, Klašnja M. 2007. Adsorption of heavymetals from electroplatingwastewater by wood sawdust. Bioresource Technology. 98(2): 402–409.

Schipper AA, Maslen MM, Hogg GG, Chow CW, Samson RA. 1996. Human infection by Rhizopus azygosporus and the occurrence of azygospores in Zygomycetes. Medical Mycology. 34(3): 199-203.

Seyfarth F, Schliemann S, Elsner P, Hiplerm UC. 2008. Antifungal effect of high- and low-molecular-weight chitosan hydrochloride, carboxymethyl chitosan, chitosan oligosaccharide and N-acetyl-d-glucosamine against Candida albicans Candida krusei and Candida glabrata. International Journal of Pharmaceutics. 353(1): 139–148.

Sobsey MC, Staube C, Casanov L, Brown J, Elliott A. 2008. A Point of Use Household Drinking Water Filtration: A Practical, Effective Solution for Providing Sustained Access to Safe Drinking Water in the Developing World. Environment Science Technology. 42 (12): 4261–4267.

Sohn S, Kim D. 2005. Modification of Langmuir isotherm in solution systems—definition and utilization of concentration dependent factor. Chemosphere. 58: 115–123.

Shimojoh M, Masaki K, Kurita K, Fukushima K. 1996. Bactericidal effects of chitosan from squid pens on oral streptococci. Journal of the Agricultural Chemical Society of Japan. 70(7): 787-792.

Subramanian A, Lin HY. 2005. Crosslinked chitosan: Its physical properties and the effects of matrix stiffness on chondrocyte cell morphology and proliferation. Journal of Biomedical Materials Research Part A. 75(3): 742–753.

Sudardsha NR, Hoover DG, Knorr D. 1992. Antibacterial action of chitosan. Food Biotechnology. 6(3): 257–272.

Taylor G. 1969. Electrically Driven Jets. Proceedings of the Royal Society A. 313: 453-475.

Troccoli NM, McIver J, Losikoff A, Poiley J. 1998. Removal of virus from human intravenous immune globulin by 35 nm nanofiltration. Biologicals. 26(4): 321-9.

Tsai GJ, Su WH. 1999. Antibacterial activity of shrimp chitosan against Escherichia coli. Food Protect. 62 (3): 239–243.

Wang H, Mullins M, Cregg J, Hurtado A, Oudega M, Trombley M, Gilbert R. 2009. Creation of highly aligned electrospun poly-L-lactic acid fibers for nerve regeneration applications. Journal of Neural Engineering. 6: 1-15.

Weicherta WS, Parkera JSL, Wahida ATM, Changa SF, Meierb E, Parrish CR. 1998. Assaying for Structural Variation in the Parvovirus Capsid and Its Role in Infection. Virology. 250(1): 106–117.

Wenten GI. 2002. Recent development in membrane science and its industrial applications. Membrane Science and Technology. 24: 1009-1025.

WHO/UNICEF JMP (Joint Monitoring Programme for Water Supply and Sanitation). 2010. Improved sanitation coverage estimates (1980 - 2010). 20-22.

WHO/UNICEF JMP (Joint Monitoring Programme for Water Supply and Sanitation). 2010. JMP Rapid Assessment on Drinking-water Quality pilot report 2010. 8-10.

Wickramasinghe SR, Carlson JO, Teske C, Hubbuch J, Ulbricht M. 2006. Characterizing solute binding to macroporous ion exchange membrane adsorbers using confocal laser scanning microscopy. Journal of Membrane Science. 281: 609–618.

Worley SD, Sun G. 1996. Biocidal polymers. Trends in Polymer Science. 4(11): 364-370.

Wu J, Wei W, Wang L, Su Z, Ma G. 2008. Preparation of uniform-sized pH-sensitive quaternized chitosan microsphere by combining membrane emulsification technique and thermal-gelation method. Colloids and Surfaces B: Biointerfaces 63(2): 164-175.

Zeng J, Xu X, Chen X, Liang Q, Bian X, Yang L., Jing X. 2003. Biodegradable electrospun fibers for drug delivery. Journal of Controlled Release. 92(3): 227–231.

Zhang CX, Yuan XY, Wu LL, Han Y, Sheng J. 2005. Study on morphology of electrospun poly (vinyl alcohol) mats. European Polymer Journal. 41: 423-432.

Zhang H, Li S, White JCB, Xin N, Nie H, Zhu L. 2009. Studies on electrospun nylon-6/ chitosan complex nanofiber interactions. Electrochimica Acta. 54(24):5739–5745.

Zhang HT, Wu CY, Zhang YL, White CJB, Xue Y, Nie H, Zhu L. 2010. Elaboration, characterization and study of a novel affinity membrane made from electrospun hybrid chitosan/nylon-6 nanofibers for papain purification. Journal of Materials Science. 45: 2296–2304.

Zhang YZ, Venugopal JR, Turki A, Ramakrishna S, Su B, Lim CT. 2008. Electrospun biomimetic nanocomposite nanofibers of hydroxyapatite/chitosan for bone tissue engineering. Biomaterials. 29: 4314-4322.

Zhang Y, Huang X, Duan B, Wu B, Li S, Juan X. 2007. Preparation of electrospun chitosan/poly (vinyl alcohol) membranes. Colloid and Polymer Science. 285: 855–863.

Zhu N, Liu W, Xue M, Xie Z, Zhao D, Zhang M, Chen J, Cao T. 2010. Graphene as a conductive additive to enhance the high-rate capabilities of electrospun $Li_4Ti_5O_{12}$ for lithium-ion batteries. Electrochimica Acta. 55: 5813–5818.

Zong XH, Kim K, Fang DF, Ran SF, Hsiao BS, Chu B. 2002. Structure and process relationship of electrospun bioabsorbable nanofiber nanofibers. Polymer. 43: 4403-4412.

7. Appendix A

Since each SEM image is represented at 2 images, this part is supplemental SEM images.
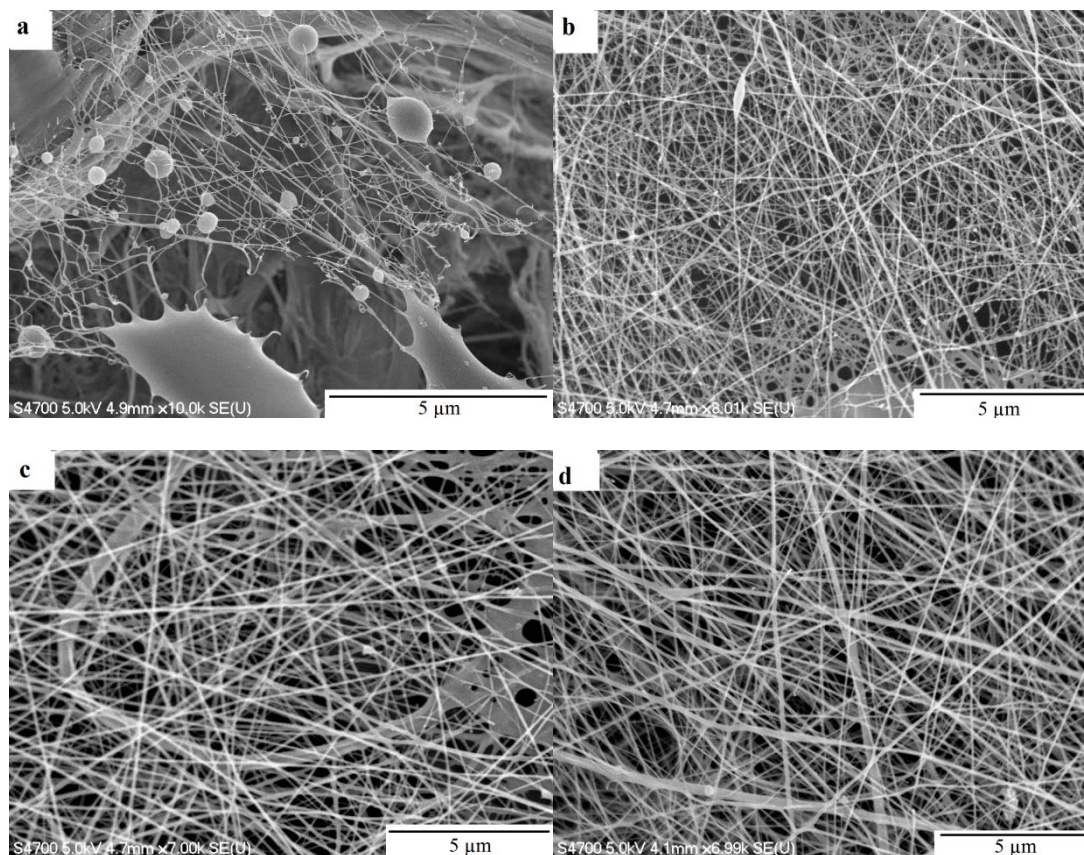
Figure 7.1 SEM images those are supplemental to Fig 4.1. SEM micrographs of electrospun chitosan/PEO in 90% acetic acid at different voltages. The mass ratio is 9:1, feed rate is 6 ml/h, concentration is 2.5 wt%, distance is 10 cm, and voltage for each sample is (a) 12.5 kV; (b) 15 kV; (c) 17.5 kV; (d) 20 kV.
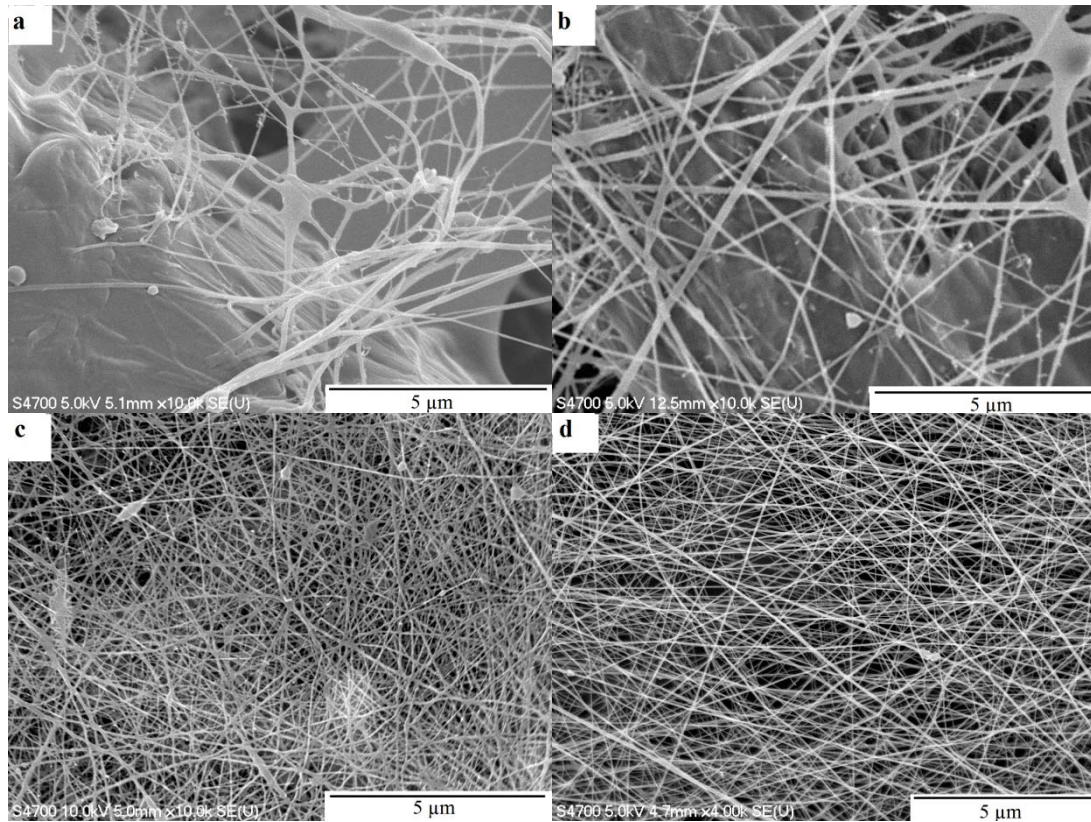
Figure7.2 SEM images those are supplemental to Fig 4.2. SEM micrographs of electrospun chitosan/PEO in 90% acetic acid at different concentration, the mass ratio is 9, feed rate, 6 ml/h, distance is 10 cm and voltage density is 20 kV. The concentration for each sample is (a) 1.25 wt%; (b) 1.75 wt%; (c) 2 wt%; (d) 2.25 wt%.
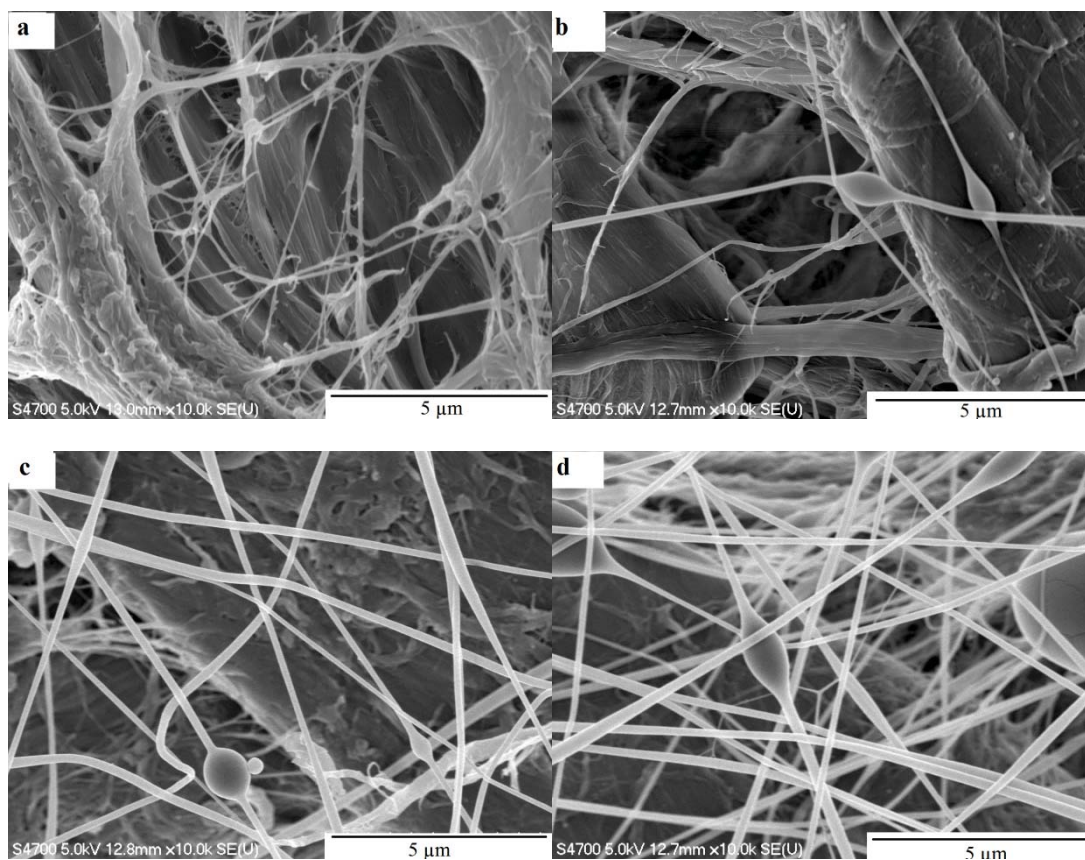
Figure7.3 SEM images those are supplemental to Fig 4.11. SEM micrographs of electrospun HTCC/graphene at various concentrations, the mass ratio is 9:1, feed rate is 6 ml/h, distance is 10 cm and voltage is 20 kV. The concentration for each sample is (a) 5 wt%, (b) 7 wt%, (c) 10 wt%, and (d) 12 wt% in water.

8. Appendix B

This part is tabulated version of results in Fig 4.3, Fig 4.4a and Fig 4.4b.

Table 7.1

Diameter of electrospun 2.5% chitosan/PEO (9:1) in 90% acetic acid nanofibers under various feed rates and voltages

Voltage (kV) / Feed Rate(ml/h)	5	5.8	7.5	9.2
15	102 nm	107 nm	111nm	118 nm
17.5	84 nm	89 nm	89 nm	99 nm
20	73 nm	82 nm	85 nm	91nm

Table 7.2

Fluorescence of two kinds of fluorescent polymers at various concentrations

C (ppm)	2	1	0.5	0.1
Fluorescence (4.6 µm)	12516	7142	4064	983
Fluorescence (1.06 µm)	22341	12293	6752	1314

Table 7.3
Beads removal of two kinds of fluorescent polymers after filtered with chitosan/PEO
nanofibers of various diameters

Diameter (nm)	Bead removal (%) of 4.6 μm particles	Bead removal (%) of 1.06 μm particles
118	63.44	35.34
111	56.81	33.69
107	53.59	32.89
102	31.76	29.89
99	31.67	26.9
91	31.07	23.15
89	29.12	22.08
89	27.32	19.98
85	26.42	17.92
84	25.05	16.68
82	24.31	14.69
73	21.19	14.33

In order to know the bead removal, those are calculated by reading the fluorescence before and after the filtration then obtain the concentration according to standard curve.

Bead removal % =
$Concentration\ before\ filtration - Concentration\ after\ filtration$

9. Appendix C

Calculation methods of virus removal

For MTT assay, make 1 blank plate, which contain just medium and MTT solution but no virus. After reading the absorbance of plates, plot a curve about absorbance (y-axis) vs. the concentration of MTT (Y-axis). Calculate CC50/ ml as the MTT concentration that is reducing 50% of the cells. One unit of MTT is equal to one unit of PPV. Since we know the concentration before and after the infection, then we can calculate the virus removal value.

$$\text{Virus removal \%} = 1 - \frac{\log(virus\ after\ infection)}{\log(virus\ before\ infection)}$$